AN ABSTRACT OF THE THESIS OF

Beate Stephan Falconer for the degree of Master of Science in Electrical and Computer Engineering presented on December 19, 1994.

Title: Grating-Tuned External Cavity Diode Lasers

Abstract approved : Redacted for Privacy

Prof. Dr. Thomas K. Plant

Diode lasers have many advantages such as small size, high efficiency and small angular dispersion of the collimated beam. However they also have some problems like lack of frequency stability. They can not be tuned in wavelength. An external cavity can solve these problems and decrease the laser linewidth.

To obtain a tunable, narrow linewidth light source, antireflection coatings were applied to commercial diode lasers which were then tested in an external cavity. Laser characteristics, such as threshold current, spectral behavior, I-V-curves, tuning range, and bandwidth were measured for the original diode laser and then compared to the measurements in an external cavity with and without antireflection (AR) coatings. The tuning range approximately doubled after AR coating. The modal stability was found to be better by a factor of 7 in the external cavity. The power amplification through the external cavity was as high as 50.

It was also attempted to process laser diodes from material fabricated at OSU, however the resulting diodes showed a high series resistance and were not usable for this project. Additional work needs to be done in this area.

The result of this work is a stable external cavity diode laser tunable over an 18 nm bandwidth which can be used as a tunable source in many applications.

Grating-Tuned External Cavity Diode Lasers

by

Beate Stephan Falconer

A THESIS

submitted to

Oregon State University

in partial fulfillment of
the requirements for the
degree of

Master of Science

Completed December 19, 1994

Commencement June 1995

Master of Science thesis of Beate Stephan Falconer presented on December 19, 1994

APPROVED:

Redacted for Privacy

Major Professor, representing Electrical and Computer Engineering

Redacted for Privacy

Head of Department of Electrical and Computer Engineering

Redacted for Privacy

Dean of Graduate School

I understand that my thesis will become part of the permanent collection of Oregon State University libraries. My signature below authorizes release of my thesis to any reader upon request.

Redacted for Privacy

Beate Stephan Falconer, Author

ACKNOWLEDGMENTS

I would like to thank my advisor Dr. Thomas K. Plant for fruitful discussions and his support. I would also like to thank the faculty members Leon Ungier and S. Subramanian as well as Don Schulte, Terry McMahon and Ming Ang for help and advice with the cleanroom procedures. My fellow students Kevin Lite, Kate Remley gave me technical support and were cheerful office mates. I appreciate that my relatives and friends did bear with me through this intense time of work, especially Maynard who helped me by taking the major load of the house work.

A special thanks to the National Science Foundation and the Cusanuswerk for financial assistance and my fellowship.

TABLE OF CONTENTS

LIST OF FIGURES

LIST OF TABLES

Table Page

GRATING-TUNED EXTERNAL CAVITY DIODE LASERS

1. INTRODUCTION

Laser diodes have become more and more popular for many every day applications such as laser printers, compact disc players and as sources for fiber optic communications. However, a serious drawback of standard diode lasers for some applications is the lack of frequency stability due to wavelength variations with drive current, fabrication aberrations and spontaneous mode hopping. Additionally, the wavelength can not be tuned. An external cavity can be a solution to these problems. It can compensate for variations and stabilize the wavelength, and the laser can then be tuned to a desired wavelength.

There has been an increasing interest in external cavity diode lasers in the last ten years[1,2,3] for narrow linewidth tunable sources and for narrow pulsewidth, picosecond sources. As improved processing facilities and refined techniques for precise thin films become more readily available, external cavity lasers become more feasible to implement.

External cavity laser diodes have the advantages of high modal stability through optical feedback, a tunable range of wavelengths, a narrow linewidth and, additionally, the capability to produce very short pulses by means of mode-locking. This is significant for a number of applications such as the optical disk head or high speed data transmission in local area networks. The configuration developed in this project can be used as a tunable source for specific applications such as:

a) atomic transition research on rubidium performed at the Physics Department of Oregon State University or

b) a project by the company Photon Kinetics to isolate problems of an Optical Time Domain Reflectometer (OTDR) by sending a range of narrow wavelengths through the fiber and extrapolating the flaws of the instrument from the results.

Other applications will be discussed in more detail later in this work.

The incentive for this research was a joint NSF (National Science Foundation) project between Prof. T. Plant at Oregon State University and Prof. M. Raymer at the University of Oregon, Eugene. It proposed a widely tunable, high gain source with narrow linewidth for use in exploring the fundamental noise limits of diode lasers. A simplified diagram of the source is shown in Figure 1.1.

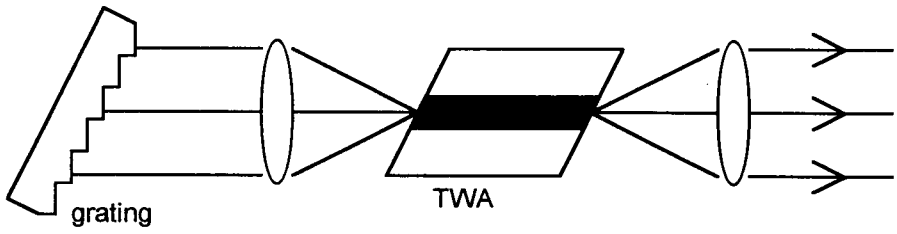

Figure 1.1.: Proposed structure with traveling wave amplifier (TWA) for studying quantum noise.

The objective of this work was to study features of an external cavity including threshold behavior, tuning range, monochromaticity, power amplification, etc., and to compare them to the features of a laser diode without feedback. This information will lead to better insight and understanding of external cavity diode lasers and can be extended to traveling wave amplifiers.

Typical diode laser wavelengths commercially available are 670, 780, 830, 1300 and 1550 nm. The wavelengths of all diodes used in this work are in the near infrared region, specifically around 780 nm. Most theoretical calculations and designs were done for 788 nm, which is the wavelength most readily available and also near the Ti-Sapphire laser optimum tuning range of 810 nm to 850 nm. Ti-Sapphire is the only widely tunable laser source in the near infra-red region and it is a solid state laser. However, an external cavity could also be designed for any other wavelength. Visibility is extremely helpful for achieving good alignment and can be enhanced by using an IR-viewer.

The power of commercially available devices is 3 to 250 mW, where the price seems to be at least exponentially related to the power. For this reason, diodes in the range of 7 to 20 mW were used.

In order to construct an external cavity laser with a reduced impact of the diode facet modes, both ends of the laser diode must have very effective antireflection coatings.

Recently, better antireflection (AR) coatings have been developed as well as better knowledge of the setup requirements and the use of different gratings to improve the overall performance of the external cavity, thus enabling new applications. A theoretical design of an antireflection coating was performed to impedance match the diode to air. This design and the results are presented.

Several different configurations were used to observe the various features of external cavity and standard semiconductor lasers. Measurements of the diode characteristics without the external cavity were taken before and after an antireflection coating was applied. The single-sided cavity was tested with three different cavity lengths to determine the effects of the cavity length on the tuning range. A double-sided cavity was used in an attempt to observe linewidth narrowing and induce single mode operation.

The following chapter will present a literature review of past and current research on external cavity diode lasers. In chapter 3, details of the active material will be described, the theoretical effects of antireflection coatings on laser operation, the effect of the tilted diode stripes and the development of the header design will all be discussed. Chapter 4 will then apply these points and show the actual outcome of tests and experiments and compare them with the expected results from chapter 3. A final chapter will be dedicated to conclusions and suggestions for additional work to further enhance this project.

2. BACKGROUND

This chapter is devoted to the background for this project. It deals with basic laser theory, and describes the design of antireflection coatings for lasers. Good antireflection coatings transform semiconductor lasers into traveling wave amplifiers, which are explained in the succeeding section. Gratings and their application in the external cavities are discussed as is the gain profile of a laser diode and its effect on the center wavelength.

2.1. LASER THEORY

A semiconductor (SC) injection laser, or a "laser diode", is a high-gain SC optical amplifier that is provided with feedback. A SC laser amplifier is a forward-biased, heavily doped p-n junction, fabricated from a direct-gap SC material. The optical feedback may be provided by gratings or mirrors, which are usually obtained by cleaving the SC material along its crystal planes. The difference in indices of refraction between two materials causes partial reflection of an electromagnetic wave traveling across the interface. Thus the SC crystal acts both as a gain medium and as a Fabry-Perot cavity. With increasing current through the diode, the gain increases and the feedback converts the optical amplifier into an optical oscillator more commonly referred to as a "laser". The lasing wavelength of a laser is determined by the spacing of two mirror ends and the band gap energy of the active material. For superposition of the waves, the length of the laser cavity has to equal an integral number of half wavelength[4]:

$$L = m \cdot \frac{\lambda_{\text{active region}}}{2} = m \cdot \frac{\lambda_o}{2\, n_{\text{active region}}}$$

The wavelength spacing between two adjacent modes is:

$$\Delta\lambda = \frac{\lambda_o^{\,2}}{2\, L\, n_{\text{active region}}}$$

Also the wavelength has to lie within the gain region (covered in section 2.6) of the diode. Therefore only those wavelengths (or "modes") will be amplified which satisfy all of the above conditions.

The laser diode (LD) is similar to a light-emitting diode (LED). In both devices, the source of energy is an electric current injected into a p-n junction. However, the light emitted from an LED is generated by spontaneous emission, whereas the light from a laser diode arises almost entirely from stimulated emission.

Three mechanisms are important to be understood in this context: induced absorption, spontaneous emission and stimulated emission. In each case, two energy levels with an energy difference of E_G (the band gap energy) are involved. In the case of spontaneous emission, an electron, excited to the higher energy level by a pumping mechanism (e.g. current injection), relaxes back to its lower energy level emitting a photon of random phase and polarization. Contrasting this, the stimulated radiation can only be created in the presence of an electron in the upper energy level **and** an incoming photon of the same energy as the transition. The electron relaxes to the lower energy state and emits a photon of the same phase and polarization as the incoming photon. Absorption is the reverse process where a photon of the transition energy approaches an electron in the lower energy level, is absorbed and the electron lifted to the upper energy level. These are idealized models of the photon-semiconductor interaction. In reality, many non-ideal effects influence the transition mechanisms.

In comparison with other types of lasers, semiconductor injection lasers have a number of advantages: small size, high efficiency, integrability with electronic components, and ease of pumping and modulation by electric current. However, the spectral linewidth of SC lasers is typically larger than that of gas- or solid state lasers.

The SC resonator length L (typically ~300 μm) is significantly smaller than that of most other lasers. Therefore, the frequency spacing ν_F of adjacent modes is large: $\nu_F = \frac{c}{2Ln}$, where c is the speed of light in vacuum and n is the index of refraction of the active medium.

There are a number advantages to the optical beam produced by a laser diode, such as:

- often nearly monochromatic emission at drive currents above threshold
  → almost no pulse distortion in fiber optic communication systems, since all the wave packets travel at virtually the same speed
- beam can be focused to a much smaller spot than the beam of a conventional light source (roughly to a spot size on the order of the light wavelength),
  → applied in technologies like CDs, CD ROM, video discs
- very small angular dispersion of the collimated beam
  → long distance optical signal transmission

Laser diodes are used in an amazing number of applications, a lot of them we handle every day or use them indirectly: CD players, laser printers, laser copiers, CD ROM, bar code scanners, facsimiles, video disc players, laser pens. Lasers are less commonly used in the following areas, but more applied in research for YAG laser pumping, medical applications, fiber optic communication sources, satellite communications, laser gyroscopes in the new Boeing 777, range finders, interferometry, strain gauges, optical disk and memory, and many more.

Along with the above advantages, some trade-offs have to be accepted. Semiconductor laser diodes are easy prey to static overcharge and breakdown. Static protection procedures always need to be applied, which proves to be a problem when loading the diodes into the evaporator for deposition of the antireflection coatings. Also, since their cavity is extremely short compared to a gas laser and has a smaller aperture, the beam leaving the cavity is not collimated as well as the one from an external cavity conventional laser. As a consequence, a collimating lens is mostly required when using laser diodes. This will appear to have quite a big influence on this project. As mentioned earlier, the wavelength can vary with differences in the processing conditions, with the intensity of the drive current and from spontaneous mode hopping. This makes diode lasers unsuitable for applications where stable single mode sources are required, like in holography, or for transition energy studies of certain materials in which the source is being tuned across the transition wavelength.

In this project, the goal is the conversion of a laser diode into a traveling wave amplifier for use in an external cavity. Since an antireflection coating transforms a laser to a traveling wave amplifier, the following section deals with thin film antireflection coatings.

2.2. ANTIREFLECTION COATINGS

Antireflection (AR) coatings are thin films. Thin films are also used in a variety of other applications like color filters, mirrors, color correction in lamps, construction of integrated circuits, storage films with magnetization and photosensitive films for computer displays. In this thesis, a commercial diode laser was transformed into a traveling wave amplifier (TWA) by applying a thin film SiO antireflection coating to both facets of the laser to prevent feedback of the optical signal.

An AR coating is a film between two media that matches the wave impedance of the input medium to the wave impedance of the output medium. This results in reduced light reflection at the interface surface in either traveling direction of the wave.

Since this project is only interested in reducing the reflectivity at one particular wavelength (which is the resonant frequency of the laser cavity) and within several nanometers around it, a simple single layer coating is sufficient. Single layer coatings can theoretically reduce the reflectivity to zero at one specific wavelength. Multiple layer coatings have a wider bandwidth, over which the impedance is closely matched, and will therefore increase the possible tunable range of the external cavity. However, multiple layer coatings make it more difficult to obtain a zero reflection coefficient. Single layer coatings provide zero reflectivity only when the wave impedances of the two adjacent materials are perfectly matched. This is the case if the coating thickness corresponds to a quarter of the wavelength in the film material and if the film refractive index equals the square root of the product of the indices of the two materials which are to be matched. It is commonly referred to as a quarter wavelength coating.

Furthermore, since the wavelength range for this AR coating is fairly narrow, one can assume the refractive index to be constant over this range. For larger wavelength ranges, the index of the thin film material would have to be determined at all wavelengths[5]. The use of AR coatings to reduce diode cavity oscillations has been discussed in many papers[6,7,8,9].

In this context, it is important to define two terms which are easily confused: the reflection coefficient ρ and the reflectivity R. The reflectivity R is the ratio of reflected to incident power while the reflection coefficient ρ refers to the ratio of the reflected vs. incident electrical field amplitude. The reflectivity is the square of the absolute value of the (possibly complex) reflection coefficient. The reflection coefficient ρ of an interface as seen in Figure 2.2.1 is given by the equation:

$$\rho = \frac{Z_s - Z_o}{Z_s + Z_o} \quad ; \quad R = |\rho|^2 \quad , \quad Z_s = \sqrt{\frac{\varepsilon_o n^2}{\mu_o}} \text{ and } Z_o = \sqrt{\frac{\varepsilon_o}{\mu_o}}$$

where Z_S is the wave impedance of the medium and Z_o, the wave impedance of air. In the same manner, one can form the equation for a thin film, that is, two interfaces.

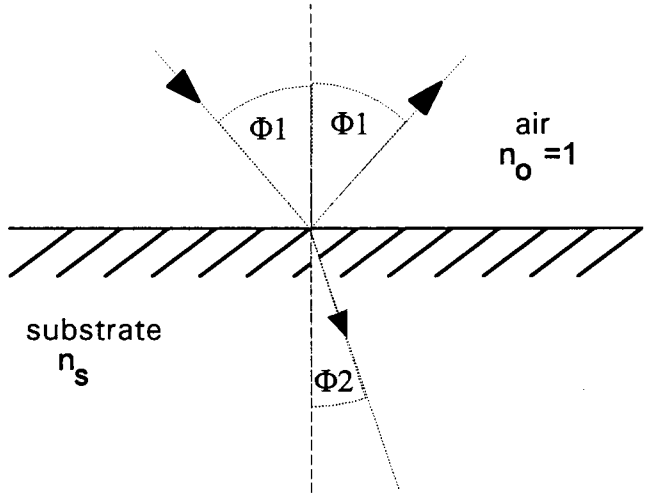

Figure 2.2.1.: Oblique incidence of a beam on an insulating substrate interface showing reflection (Φ_1) and refraction (Φ_2).

The formulas are complex[10]; however, for normal incidence they can be significantly reduced. Expressing the complex reflection coefficient ρ in terms of the indices of refraction, one obtains:

$$\rho = \frac{n_2 \cos(kl) + i\, n_3 \sin(kl) - n_2 (n_3 \cos(kl) + i\, n_2 \sin(kl))}{n_2 \cos(kl) + i\, n_3 \sin(kl) + n_2 (n_3 \cos(kl) + i\, n_2 \sin(kl))} \text{ where } k = \frac{2\pi n_2}{\lambda_o} .$$

k is the wave vector or the eigenvalue of the wave solution, λ_o is the free space wavelength and, in the case of a thin film coating, n_3 and n_2 are the substrate and film indices, respectively. Without a coating, the diode has a "natural built-in" mirror, the semiconductor-air interface. It has a reflection coefficient of:

$$\rho_{AlGaAs} = \frac{n_s - 1}{n_s + 1} = \frac{2.5}{4.5} = 55.5\%$$

or, in terms of reflectivity, R= 30.86 % at normal incidence, where n_S is the index of refraction of the active medium AlGaAs of the diode. ρ is the more general form and was used in the theoretical design of the AR coatings (see below), but the measurable quantity is the power intensity. Thus we will refer to the power reflectivity R from here on. The optical power is related to the square of the electrical field intensity by:

$$P = \frac{1}{2}\frac{|E|^2}{\eta_o}$$

where ηo is the free space impedance. In all power measurements, as in the P-I-curves, the power was measured with a Newport Digital Power Meter, Model 815.

The following table shows the refractive indices for GaAs, AlAs and $Al_XGa_{1-X}As$, where the aluminum concentration x equals 12%. The aluminum concentration can be extracted from a linear approximation of the two composite materials GaAs and AlAs.

Material	Index of refraction
n (AlAs)	3.178
n (GaAs)	3.59
n ($Al_xGa_{1-x}As$) where x = 12 %	3.5

Table 2.2.1.: Indices of refraction of typical laser materials (x = aluminum concentration)[11].

The aluminum concentration x can also be calculated from the energy gap (or resonating wavelength) using an equation given by Casey and Panish[11]:

$$E_G(Al_xGa_{1-x}As) = (1.424 + 1.247 \cdot x)\ eV$$

The energy of an emitted photon can also be approximated by:

$$E_G = \frac{1.24\ \text{eV}}{\lambda\,[\mu\text{m}]} \quad \text{from} \quad E = \frac{hc}{\lambda}$$

If a thin film is applied onto the semiconductor, the reflectivity can be reduced significantly, in the ideal case to zero. A perfect antireflection coating would be a film of quarter wavelength thickness and an index of refraction n_f equal to $\sqrt{n_s}$, and for the above AlGaAs:

$$n_{film} = \sqrt{n_{air} \cdot n_{substrate}} = \sqrt{1 \cdot 3.5} = 1.8725$$

$$d = \frac{\lambda_f}{4} = \frac{\lambda_o}{4n_f} = \frac{788\ \text{nm}}{4 \cdot 1.8725} = 105.2\ \text{nm}$$

For the case of an imperfect coating, the change of reflectivity with thickness of the layer and with refractive index of the layer has been calculated. (For the MATLAB script of "coating.m", please refer to Appendix 1.)

The output of the program "coating.m" (see Figure 2.2.2) is divided into four parts. The first graph (top left) shows the absolute value of the reflection coefficient ρ as a function of film thickness. The first time ρ becomes zero is at 1052 Å when a film of a quarter wavelength thickness has been deposited. The function is periodic with a period of pi and so are the real (top right) and imaginary parts of ρ (bottom right). The reflectivity (bottom left) starts with a value of 30.86 % and also zeros at 1052 Å. A deviation in coating thickness will only result in a small deviation in reflectivity, since the curve is fairly flat around its extreme values.

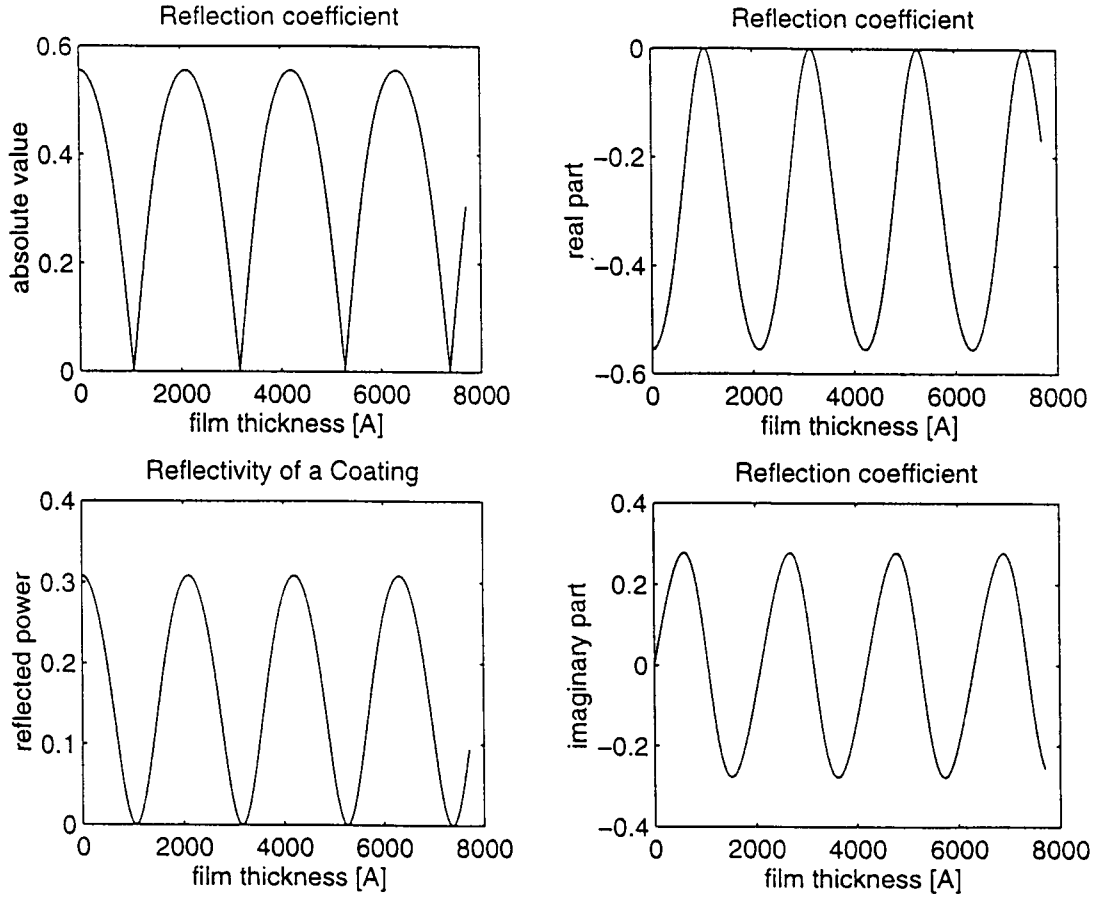

Figure 2.2.2.: Output of the MATLAB program "coating.m".

The program called "threshold_refl.m" (see Appendix 1) calculated the threshold behavior of a laser diode. It produces four plots also displaying the threshold current density vs. the product of the reflectivities of both facets (top left) and vs. coating thickness (top right). Multiplying by the area (here shown for an area of 75 000 sq. microns corresponding to a typical Sharp laser diode), one obtains the threshold current (bottom left). This again is for a diode with initial threshold current of 40 mA. Unlike the reflectivity, which does not change much with a small error in coating thickness, the threshold current shift is very sensitive to even minute errors in the thickness. In the ideal coating case the threshold should be pushed out to infinity. An error of 5 % in thickness will decrease the threshold shift to 60 mA or below. The graph on the bottom right simulates the optical power output as measured for all diodes as "P-I-curves". The equation used is given and discussed in section 4.2.

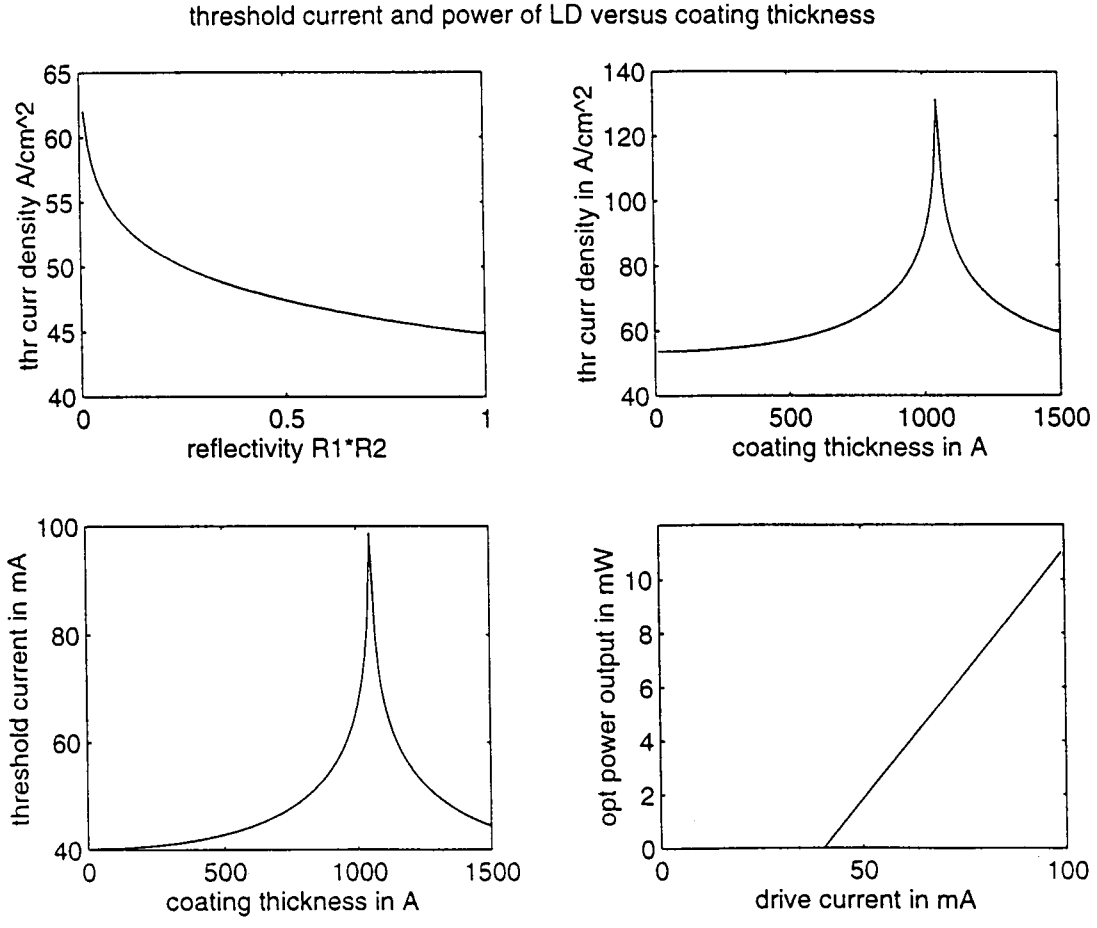

Figure 2.2.3.: Output of the MATLAB program "threshold_refl.m".

2.3. TRAVELING WAVE AMPLIFIERS

There are several different configurations of SC diode optical amplifiers such as reflected wave amplifiers, traveling wave amplifiers (TWAs) and funnel amplifiers.

A reflected wave amplifier is a laser diode with an AR coating on one facet and a high reflectivity (HR) coating on the other. The input signal enters the AR coated end, travels through the gain medium, is reflected off the HR facet, and passes through the gain medium again before exiting the amplifier.

A traveling wave amplifier amplifies the injected light ideally in one single pass. The amplification must be large enough to raise the incoming signal above the system noise level. TWAs play an important role in fiber optic communications where the signal decreases in amplitude while traveling along the long distance fiber and needs to be periodically amplified to remain above the noise level for accurate detection in the receiver. TWAs provide gain if under forward bias, so the light gets amplified in one single pass, and in the ideal case the light is not reflected at the ends of the resonating cavity.

A funnel amplifier is basically a traveling wave amplifier whose shape is tapered such that the top view looks like a funnel. With this kind of SC amplifier, a much higher output power can been achieved[12].

Traveling wave amplifiers are currently being used in a current joint NSF (National Science Foundation) project of Prof. T. Plant at OSU with Prof. M. Raymer at the University of Oregon, to study fundamental quantum noise limits in semiconductor laser amplifiers.

2.4. GRATING THEORY

In order to prevent multiple longitudinal modes from lasing and to allow tuning of the laser output, one of the reflectors must be a frequency selective element - usually a diffraction grating. This section explains the general operation of a diffraction grating and its application to the external cavity laser.

The most straight forward way to describe a (ruled) diffraction grating (see Figure 2.4.1) is by modeling it using an array of N identical apertures or slits. For example, a 1200 lines/mm grating would correspond to a row of elongated apertures with equal spacing of d = 0.8333 μm. The light is refracted from the grating in the same manner as it would be transmitted through a line of narrow apertures. Figure 2.4.1 shows the incoming as well as the refracted beams in a Littrow configuration. Littrow is a special grating position in which the incoming beam is at an angle Θ to the perpendicular axis of the grating plane which equals the grating blaze angle Θ_B. This results in the mirror reflection from each facet returning on the path of the incoming ray.

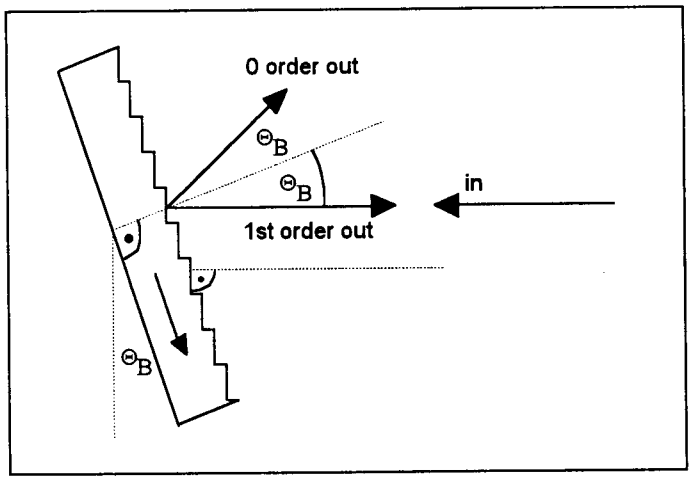

Figure 2.4.1.: Ruled diffraction grating indicating the angles perpendicular to the facets and perpendicular to the grating plane as well as the zero and first order refracted beam in a Littrow configuration.

The diffraction grating used in these experiments is 12.5 x 25 mm in size, has 1200 grooves per mm and has a blaze angle of 26°44' at the design wavelength of

750 nm. The diffraction efficiency, given by the manufacturer, lies between 60 and 80 % at the design wavelength. Measurements found results close to these values. LD 19, a Sharp LT031MD0 device, was used here, since its center wavelength is exactly the blaze wavelength of 750 nm. With the beam polarized perpendicular to the grating grooves, an efficiency of 77.5 % was observed, while with the polarization parallel to the grating grooves, an efficiency of 43 % was detected. The latter result may be low, because the total laser intensity with this orientation of the polarizer was very small.

The same measurement for an unblazed holographic grating of 1800 grooves per mm showed efficiencies of 69.7 % and 10.5 % for the perpendicular and parallel polarization directions, respectively.

All of the above tests of the blazed grating were taken in the Littrow configuration. Another possible configuration for external cavities besides the Littrow configuration is called "grazing incidence" configuration, because the beam hits the grating at a very flat angle, or in terms of Θ, a very large angle Θ. In all external cavity designs for this work, however, the Littrow configuration has been used, since the literature suggests that this is the more stable system[13]. By providing feedback with the grating, only one specific wavelength is reflected directly back down the cavity path. At other wavelengths the cavity loss will be greater and thus the diode will lase at only the tuned wavelength. By changing the grating angle, a different wavelength will be reflected back down the cavity path. The diode will then lase at this new wavelength. Gratings have been used in this project for tuning the wavelength of the external cavity in the above manner.

2.5. EXTERNAL CAVITY LASERS

An external cavity (EC) is basically a traveling wave amplifier (TWA) with feedback, which can be provided from either mirrors or gratings or by an uncoated facet of the diode. The TWA is the gain material in the configuration, the mirrors or gratings form the external Fabry-Perot cavity. The most basic external cavity is shown in Figure 2.5.1.

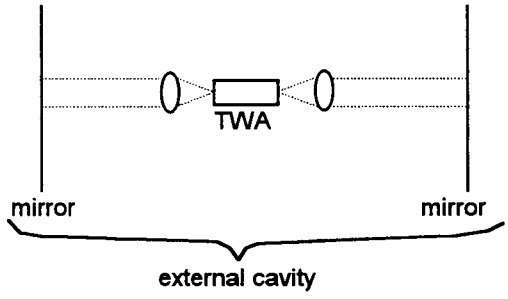

Figure 2.5.1.: Basic external cavity cell consisting of a traveling wave amplifier and two mirrors as the external Fabry-Perot cavity. Lenses are required to collimate the expanding laser beam.

There are several reasons, why scientists are trying to develop good external cavity laser diodes:

- An external cavity is capable of producing very short, sharp pulses in the range of picoseconds by means of mode-locking. The narrower a single pulse is, the higher is the possible data transmission speed and the more data can be transmitted in the same amount of time in a local area network (LAN). However, in long distance communications extremely short pulses are not desirable, because they contain a broad range of frequency components and therefore the dispersion of the pulses would be high[14,15,16].
- The external cavity provides high modal stability through optical feedback; mode hopping is severely reduced compared to a conventional laser diode[17,18]. Stable, single-frequency sources are very necessary for fiber optic communications where 1.3 μm is the minimum dispersion wavelength of the fiber and 1.55 μm is the minimum loss wavelength, but has higher dispersion. The better the mode rejection

ratio, the lower the dispersion. The mode rejection ratio is defined as the ratio of the intensity of the dominant mode to that of the next most intense mode[19]. This ratio is excellent for external cavity lasers, distributed feedback lasers and cleaved-coupled cavity lasers.

- The tuning range of the resonating wavelength in the Fabry-Perot cavity - also referred to as wavelength controllability - is desirable for a wide range of applications one of which is wavelength division multiplexing [1,20]. Tuning ranges which have recently been reported reach from 30 to 55 nm and in the case of a tapered waveguide 200 nm[21] by using several gain elements. Moreover, it introduces the option of easily changing the cavity-Q by adjustment of the length. The Q-factor is related to the finesse which measures the resolution of a cavity. Thus a higher Q results in a better resolution.
- A very narrow linewidth can be obtained by coupling a laser diode to an external cavity[22]. This supports the previous point in allowing close spacing of the modes for wavelength division multiplexing. It also provides less dispersion, since the frequency range of the signal is very narrow.
- Difference-frequency-mixing and frequency-doubling are possible by means of an external cavity [21].

There are many possible applications of external cavity diode lasers. Short pulses and tunable, narrow linewidth CW sources are both useful in communications and spectroscopy. Spectroscopy helps determine fluorescence, index of refraction and other material properties. As already mentioned, wavelength division multiplexing transmission systems are a good field for applying the feature of wavelength controllability[23]. As many as 200 channels have been achieved or 10 channels with 668.25 Mb/s in large capacity or high speed, coherent optical signal transmission systems, respectively [1]. High power and coherency have been accomplished by coupling multiple gain elements together by an external cavity[24]. An interesting device with an external cavity laser is the fiber optic velocimeter [23].

The use of external cavities as a sensor mechanism opens a completely new direction of applications. They have been applied as displacement sensors to measure acoustic and magnetic field strength[25], as distortion sensors[26], and in an optical disk signal detector as a reflectivity sensor[27]. EC diode lasers are also used for holography where a narrow linewidth gives a long coherence length and, thus, a greater depth of field. For all of these applications a good understanding of the behavior of external cavities is required.

One phenomenon which should be explained in this context is the lowering of the threshold[28] with external feedback from a grating. Figure 2.5.2 illustrates this clearly. The gain curve resulting from the distribution of the carriers and the loss line caused by the facet losses of the Fabry-Perot cavity of the SC diode determine the threshold condition. Only where the gain is larger than the loss will light experience amplification. When a grating is introduced into the cavity, one particular wavelength is reflected into the gain material with an efficiency as high as 80% - depending on the grating efficiency - while all other wavelengths do not re-enter the diode and therefore experience loss.

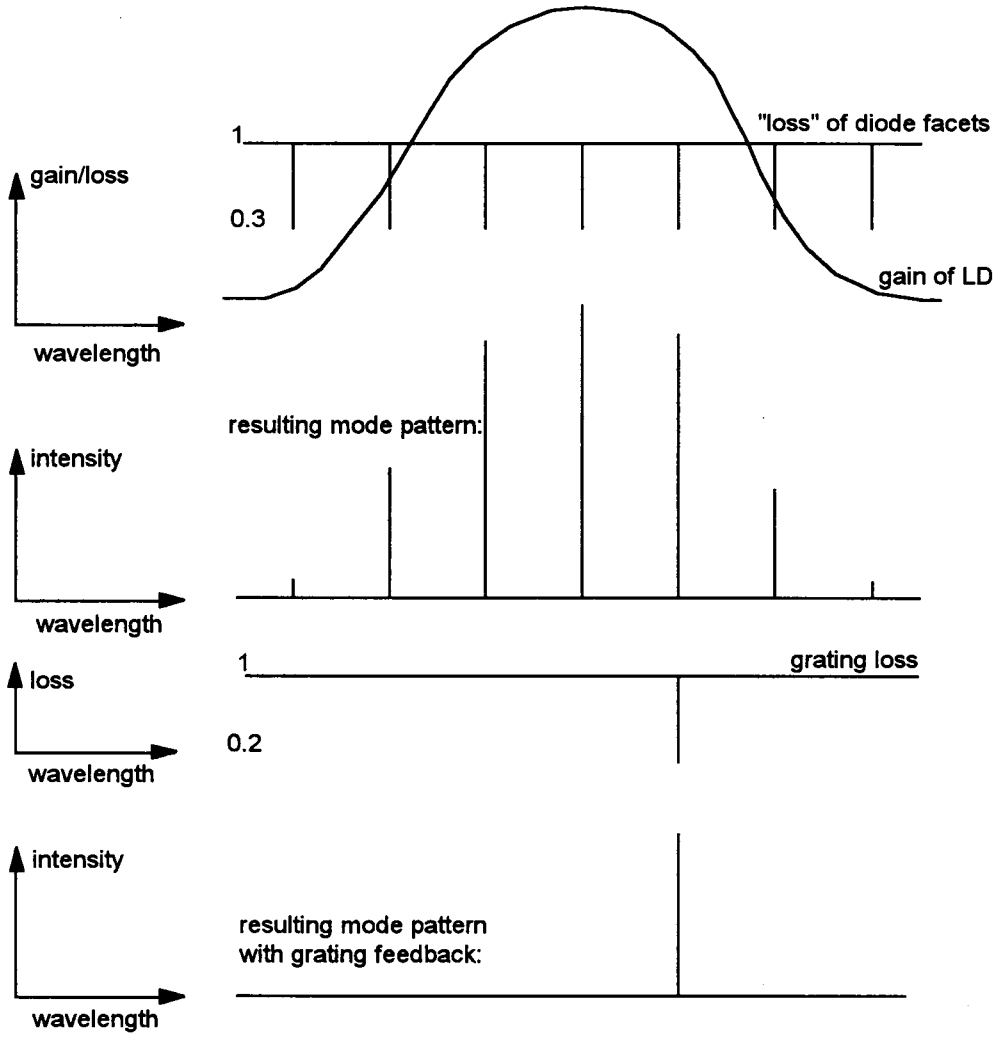

Figure 2.5.2.: Gain and loss in a laser diode and external cavity and resulting mode patterns.

In other words, this wavelength experiences feedback due to the grating while all other wavelengths do not. The resulting mode pattern is a single mode spectrum as seen in the last part of Figure 2.5.2. It could be said that the grating effectively increases the reflectivity of one facet for the particular wavelength to which it is tuned. This concept will be important later on when the AR coatings will influence the "loss".

External cavities have been built at various lengths from several μm[25] up to 3 meters[2] in a ring laser cavity. The standard length however is around 10-30 cm.

For good coupling it is necessary to provide precise orientation of the external mirror. A tilt angle bigger that 5 μrad decreases the efficiency of the external cavity and lowers the power output[18].

2.6. GAIN CURVE AND CENTER WAVELENGTH

The external cavity is able to stabilize the center wavelength and manipulate the gain/loss curve. Hence, the reasons for "natural" shift of the diode wavelength and the impact of electrical pumping on the gain curve as well as the connection between the two will be explained in this section.

The gain curve of a laser diode is brought about by the distribution of the carriers in the conduction and valence bands. The number of transitions with equal wavelength between conduction and valence band render a curve that is approximately Gaussian when plotted versus wavelength, the gain curve.

In Figure 2.5.2 in the previous section, we have seen the mode pattern of a regular SC diode laser. The Fabry-Perot (FP) modes closest to the center of the gain curve obtain the most light amplification and, hence, the largest intensity. Above threshold, this mode becomes several orders of magnitude larger than its neighbors and is called the center wavelength or "lambda zero" λ_o. This quantity is usually given with a nominal value on the package of commercial LDs. However, the lasers do not always lase at the nominal wavelength. Small variations in their manufacturing can shift the wavelength by a small amount. Here an external cavity can solve the problem, if one needs a specific wavelength, by tuning the wavelength up or down from the offset wavelength.

But not only manufacturing can alter the center wavelength. Heating effects in the semiconductor during the time of operation can cause the wavelength to shift, too.

First of all, the index of refraction n of the active region is slightly dependent on temperature. This can alter the FP modes, since:

$$\Delta\nu = \frac{c}{2n_{a.r.}L}.$$

Secondly, a heating of the diode changes its length. As the FP cavity expands, a mode of a different wavelength now satisfies the condition that the cavity length must equal an integral number of half wavelengths or:

$$L = m \cdot \frac{\lambda_{a.r.}}{2} = m \cdot \frac{\lambda_o}{2n_{a.r.}}.$$

For example, the linear thermal expansion coefficient $\frac{\Delta L / L}{\Delta T}$ of GaAs is 6.86 E-6 /°C. This corresponds to an expansion of 2.058 nm per degree Celsius for a 300 μm long semiconductor cavity.

Furthermore, pumping the diode harder, i.e. using a higher drive current, alters the gain profile. Harder pumping means an increase in the energy of the electrons or in other words a shorter wavelength. Hence, the center wavelength shifts towards shorter wavelengths. An increase in drive current additionally heats the diode if no means of cooling are applied. From these explanations, one can see why wavelength stabilization is important for applications which require specific stable wavelengths.

3. DESCRIPTION OF APPLIED METHODS

This chapter will deal with the active material and its properties, its characterization by photoluminescence, the transformation of the laser diodes into traveling wave amplifiers by means of antireflection coatings, and it will also describe the development of the design of appropriate headers.

3.1. THE MATERIAL

The commercial diodes from Sharp and Mitsubishi are made from AlGaAs, which is a ternary alloy, that is, it consists of three elements. The substrate is GaAs, a III-V compound semiconductor from gallium and arsenic. GaAs is a direct band gap semiconductor which has a great advantage for optical applications: virtually all of the transition energy is converted to light unlike in indirect materials where some energy is lost to lattice vibrations (phonons). Silicon is an example of an indirect band gap material. This is the reason that all laser diodes are made from direct band gap semiconductors.

AlGaAs and GaAs are frequently used in combination, since their lattice constants match very closely. The lattice constant is the minimum distance after which the lattice pattern in a crystal is repeated, that is the length of a basic lattice cell. Therefore no strain is created when growing one material on top of the other. If a material of a different lattice constant was used, its lattice would be stretched or compressed when growing on the substrate. Those materials are called strained layer materials. The close lattice match of AlGaAs and GaAs makes predictions about the behavior of the material easier, since there are many mechanisms involved with strained materials, which are not completely understood up to now.

3.2. ANTIREFLECTION COATINGS

It is possible to build an external cavity laser without an antireflection coating, but this would result in parasitic oscillations from the diode cavity. Therefore it is of advantage to apply an antireflection coating on one or both sides of the semiconductor diode. If a thin film of index n_F is applied onto a semiconductor of index n_S, the reflectivity can be reduced significantly, in the ideal case to zero. The ideal antireflection coating would theoretically be a film of quarter wavelength thickness and an index of refraction n_F equal to the square root of n_S.

The antireflection coatings were deposited by means of thermal evaporation of silicon monoxide (SiO). SiO has an index of approximately 1.9 at 788 nm, which corresponds closely to the square root of the product of the indices of air and AlGaAs.

Bulk SiO has a density of 2.13, an evaporation temperature of 1100° C and it sublimes, that is, it vaporizes without melting. Most oxides show this phenomenon. SiO should be evaporated from tungsten (W) or tantalum (Ta) boats or by electron beam evaporation. In the visible range SiO has a refractive index of 2.0. In the infrared region the index decreases to 1.7. The typical applications of SiO are protective films for front surfaces of aluminum mirrors, low index layers for infrared filters or multi-layers[29].

For evaporation, SiO chunks were loaded into an alumina (Al_2O_3) covered tungsten boat. High current (about 125 Amps) heats up the film material. The molecules move with high speed towards their target and build a thin film. The evaporation takes place in a vacuum chamber at pressures of 10 E-7 to 10 E-6 Torr.

During the evaporation process the deposited film thickness is monitored by a quartz crystal resonator, so that the current can be shut off when the desired thickness of 1052 Å is achieved. Afterwards the thickness was checked with an ellipsometer by measuring a reference sample that was positioned next to the diode laser. It was found that often the thickness differed from the one determined by the film thickness monitor, since 50 Å is about the resolution of the monitoring instrument.

Ukita et. al.[30] developed a formula for determining the reflectivity of a coated laser diode just by geometry and the ratio of old and new threshold current. The reflectivity can easily be calculated from Ukita's formula:

$$\log_{10} R_2 = -1.545 \frac{I_{th}}{I_{th,o}} + 1.050 ,$$

where R_2 is the reflectivity of the coated facet, I_{th} is the threshold current after evaporation and $I_{th,o}$ is the initial threshold current.

Taking the P-I-curve is a standard procedure for this project and the threshold current can be determined from these curves. However, this equation is based on the assumption, that the LD cavity length is 250 μm, while the diodes used in this project were about 300 μm long. After extrapolating the two constants and compensating for the 300 μm, the equation becomes:

$$\log_{10} R_2 = -1.656 \frac{I_{th}}{I_{th,o}} + 1.161 \qquad (1)$$

so that for some example evaporations the approximate facet reflectivities are:

	I_{th} before evap.	I_{th} after evap.	facet reflectivity R
diode #1	39 mA	58 mA	4.30 %
diode #2	38 mA	65.5 mA	2.13 %
diode #9	42 mA	72 mA	2.10 %
diode #12	40.2 mA	60 mA	4.89 %

Table 3.2.1.: Threshold currents and facet reflectivities of some coated laser diodes.

According to Ukita's compensated equation (1), a diode of 788 nm and an initial threshold current of 40 mA would have to shift to 75.4 mA for a reflectivity R_1 of 1 % or to 83.6 mA for R_1 = .5 %. The results of the coatings will be discussed further and compared to other measurements in chapter 4.2.

An alternative method to the conventional thermal evaporation would be to deposit a PECVD (**P**lasma **E**nhanced **C**hemical **V**apor **D**eposition) film. It has been shown by former students, that the PECVD system can be used at room temperature to prevent heating the diode too much and melting its solder bond to the header. However, the trade-off is that the film is not very rugged. PECVD is a thin film deposition process whereby diluted reactant gas is introduced into a heated reaction chamber, transformed into a plasma by a radio frequency power supply which collides with the substrate surface where the atoms form a thin film. With PECVD, the index of refraction can be selected within a range of 1.46 and 2.0 (at 632.8 nm) and the thickness of the layer is easily controlled, so that it should be possible to hit very close to the ideal coating conditions.

3.3. TILTED ANGLE DIODES

It is not always possible to obtain a perfect antireflection coating. For one thing, the thickness read from the quartz thickness monitor during the evaporation process and during the cooling period afterwards varies with temperature and pressure, so that cooling the film substrate before unloading it and releasing the pressure before opening the chamber will cause the thickness reading to change. Another contributing factor is that the index of refraction of the SiO film is not exactly matched to the effective laser index at the lasing wavelength of 788 nm.

There are two reasons for this. First, the refractive index of bulk SiO should be exactly equal to the square root of the effective index in the active region of the laser. This is a property of the SiO material which cannot be changed. Second, even if the bulk index were correct, the index of the evaporated thin film can vary slightly from the bulk index due to differences in film density and composition.

Finally, Eisenstein[31] has shown that the "ideal" thickness deviates from $\lambda/4$ due to the Gaussian beam shape wavefront of the beam leaving the laser facet.

Since there will always be some small residual reflectance at an AR coated facet, another method was found to further reduce the surface reflections. If the active stripe contact of the laser diode is tilted at a small angle to the cleaved mirror facets, the reflected portion of the beam will no longer be phase matched for Fabry-Perot resonance and will not cause an interference in the output. Angles between 4° and 6° are commonly used. It was decided to use an angle of 5.8° on the devices to be fabricated here at OSU.

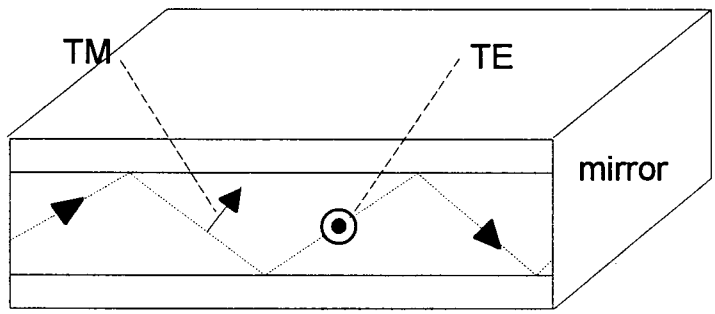

Figure 3.3.1.: Laser diode slab showing the waveguide layers and a ray with its TE and TM components. The arrows of TE and TM are indicating the directions of polarization of the respective electrical fields.

The transverse electric (TE) and transverse magnetic (TM) waves (see Figure 3.3.1) traveling in a waveguide (here the laser active medium) have different reflection coefficients. Since in laser diodes TE is the dominant mode, i. e. the mode with the higher intensity, it is more important to design the coating such that it reduces the reflectivity of the TE mode. We have fabricated tilted stripe devices in the MBE material to show it is possible, however, further work on this design is postponed until after successful laser processing. Tilted stripes will be used for the high-gain saturating TWAs made for the NSF grant.

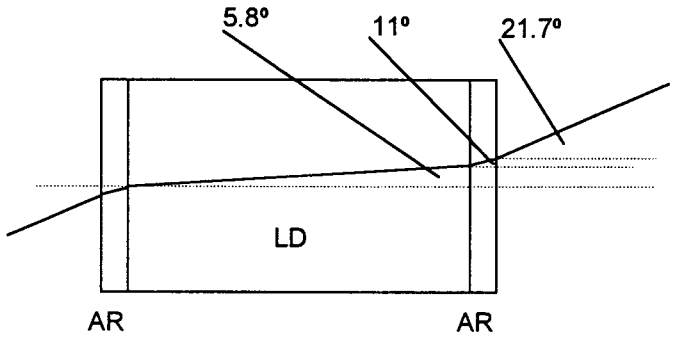

Figure 3.3.2.: Top view of a tilted stripe laser diode (LD) with antireflection coatings on both facets indicating the beam path through all media according to Snell's Law.

3.4. DIODE HEADER DESIGN

As this project developed, so did the requirements for new headers used for remounting the commercial lasers and for mounting the OSU devices. The requirements are as follows:

- wide access to the lasing facets for unrestricted light emission, minimal reflections and smooth coatings of the second facet
- side shoulders to attach the gold plated alumina contact pads and the ground contact
- good heat conduction capabilities to function as a heat sink
- side panels to provide room for screw holes to attach the header to a bigger heat sink
- rugged and easy to handle
- design must be compatible with wire bonder and die attach schemes.

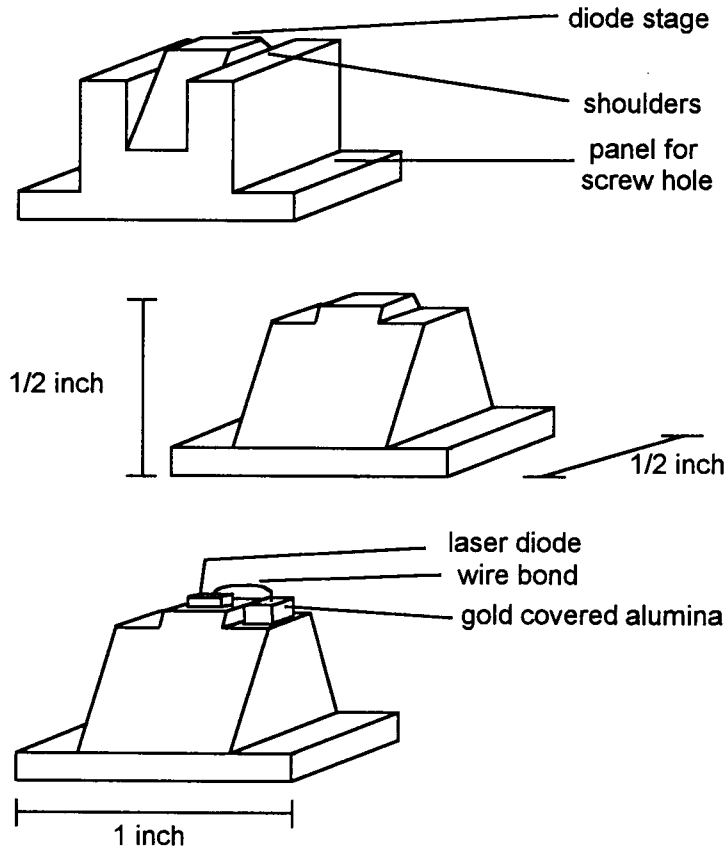

Figure 3.4.1.: Design of diode headers/heat sinks for remounting a (top): initial design, b (middle): improved design, c (bottom): header with diode mounted.

The first headers built can be seen in Figure 3.4.1.a. Unfortunately, the wide shoulders did not allow close proximity of the small collimating lenses (focal length of 1-2 mm) to the diode facets. Therefore the variation shown in Figure 3.4.1.b was fabricated.

Since packaging and remounting of the commercial diode lasers was a large component of this work, it will be briefly described here. The designed headers had been fabricated by OSU and altered manually as different requirements occurred. The laser diodes were fastened to their new mounts by several means: colloidal silver adhesives (also called "silver epoxy"), indium solder or indium tin solder (52% In, 48% Sn). Silver epoxy has the advantage over indium solder that it tends not to leave particles on the front and back lasing facets. On the other hand, the controllability of the indium solder staying liquid and its feature of forming very thin films on the copper mount shoulders were preferable over silver epoxy. The indium tin solder (In/Sn) has a lower melting point than pure indium (In). The melting point of In/Sn is 118° C. A low melting point is desirable to prevent the alumina contact pads (bonded with "super-glue") from coming off the header.

Once the diodes were on the new mounts, electrical contact was made. A gold wire-bond was made from the gold plated alumina contact pad to the top of the diode. The alumina layer provides electrical isolation of the p-contact from the mount which served as the n-contact. For the gold wire-bonds, a Mech-El Industries Wirebonder Model 827 with temperature controllable bonding stage was used. The temperature on the stage can be varied from 0-799° C. Indium solder melts at about 150° C and silver epoxy cures in 60 minutes at 200° C. Wire-bonding is usually done at about 100° C. However, to prevent any movement of the diode, it was performed at room temperature. As it turned out, the bonds were just as good as the higher temperature ones.

3.5. EXTERNAL CAVITY SETUP

As mentioned earlier, an external cavity laser is a TWA - serving as the gain material - with external feedback provided from either mirrors or gratings or by the uncoated facet of the diode. Several setups were tested.

3.5.1. Diffraction gratings

Two different gratings from Edmond Scientific were examined in the setup, a ruled diffraction grating and a holographic diffraction grating (see table 3.5.1.1). The ruled grating has the advantage of higher peak efficiency. Its peak reflection efficiency is 60-80%, while the holographic grating has a maximum reflection efficiency of 45-65%. The advantage of the holographic grating over the ruled one is that of higher resolution and more uniform response. Ruled gratings can be fabricated with 1200 - 1800 groves per mm. Holographic gratings can be made with up to 3600 grooves per mm. In this case, an 1800 groves/mm holographic and a 1200 groves/mm ruled grating were examined. Since a high feedback and thus a high reflection efficiency are needed, the diffraction grating was used in most cases.

grating type	size[mm]	grooves/mm	optimum wavelength	pattern
ruled grating	12.5 x 25	1200	750 nm	26°44' blaze
holographic grating	12.5 x 25	1800	VIS	sinusoidal

Table 3.5.1.1.: Grating types and their parameters.

The blaze angle Θ_m is the angle at which the m-th order ray is reflected from the grating. In the case of Figure 3.5.1.1 the zero-order output is shown, while the first order beam is reflected back along the input beam, or in the case of an external cavity

application, back into the laser diode. The 1200 grooves/mm grating is designed for 750 nm with a blaze angle of about 26°44'. This angle will deviate slightly for the investigated wavelength of 788 nm.

The equations next to the figure describe the reflection optics in a more detailed way. For a light source of 788 nm center wavelength, the first order reflected beam will reflect from the ruled grating at 28.2°. For the holographic grating, the equivalent angle will be 45.2°.

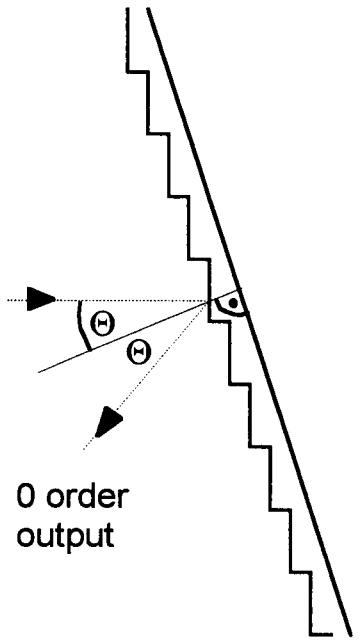

$$m\lambda = 2d \sin\Theta_m$$

$$d = \frac{1}{1200 \cdot 10^{-3}}\,\mu m = 833.3\ nm$$

$$\sin\Theta_m = \frac{m\lambda}{2d} \Rightarrow \Theta_1 = 28.2°$$

for 788 nm and 1200 grooves / mm

$\Theta_1 = 45.2°$ for 1800 grooves / mm

Figure 3.5.1.1.: Diffraction grating and ray optics displaying the blaze angle Θ and the zero order output with the first order output returning into the same path as the input beam comes from.

To make the emitted radiation of this laser visible, a special viewer, called a "FInd-R-scope", was used. The FInd-R-scope is an image intensifier in which the photo electrons from the cathode are accelerated through a high electric filed, focused by an electrostatic lens and then strike a phosphor screen creating a visible luminescent image.

3.5.2. Single sided cavity with a grating output

In this configuration shown in Figure 3.5.2.1, one grating was used and no mirror or AR coating on the second side. The ruled diffraction grating in a Littrow configuration was used for this setup. In the case of the uncoated diode, three cavities are formed: one between the grating and the back side of the diode (external cavity), one between the grating and the front facet of the diode (parasitic cavity), and the third one is the Fabry-Perot cavity of the SC diode itself (LD cavity). The parasitic cavity results from the 30 % reflectivity of the front facet before coating or from the small remaining reflectivity after coating.

Light was emitted from the LD and collimated onto the grating by an AR-coated aspheric laser diode collimating lens of design wavelength 780 nm and focal length f = 4.5 mm by Optima Precision. The first order reflection from the grating was coupled back into the diode, while the zero-order reflection was directed to the measuring monochromator by a mirror and a fiber bundle. The first order reflection of a grating is the strongest in power and therefore gives the strongest feedback.

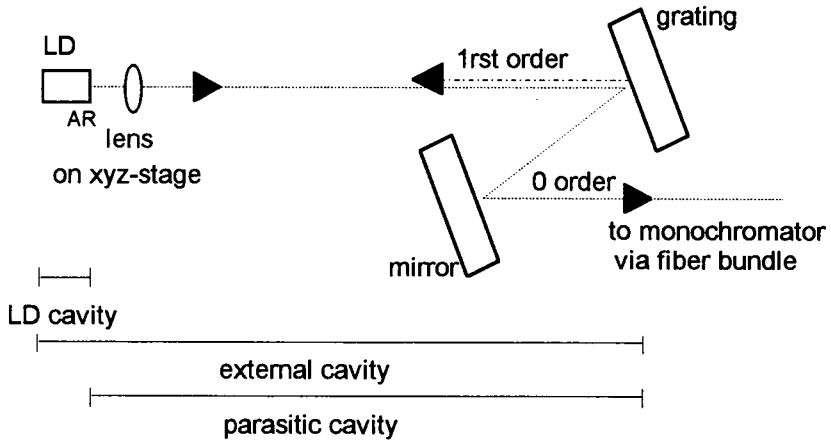

Figure 3.5.2.1.: Single sided cavity setup with a diffraction grating and AR coating on one side.

The light emitted from the second side was lost to the signal amplitude. The performance and efficiency of this setup could be immensely improved by furnishing the back side of the laser diode with a high reflectivity coating.

3.5.3. Double sided cavity with mirror and grating

In this configuration, one mirror and one grating were used. The mirror and the grating form the external cavity, while in the single-sided configuration the grating and the uncoated laser facet formed the external cavity.

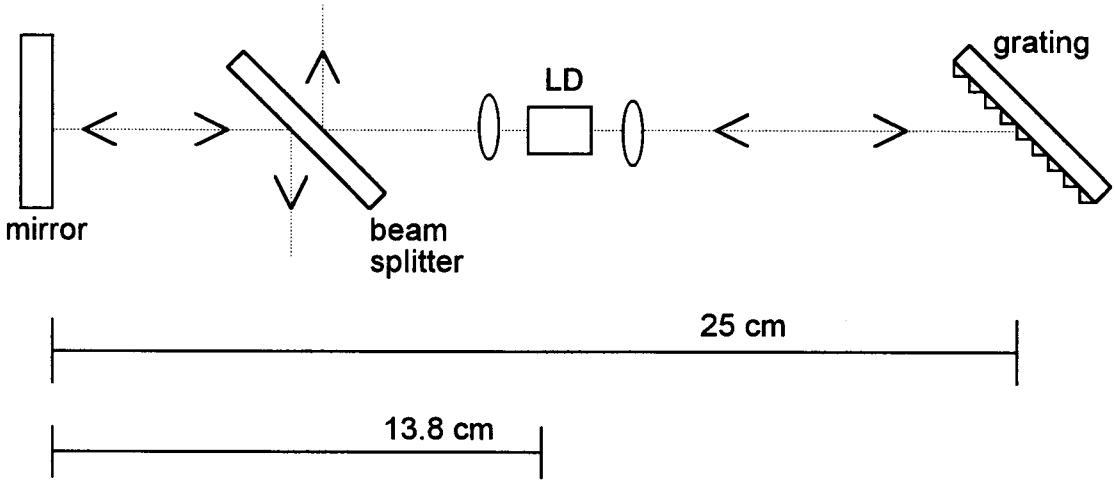

Figure 3.5.3.1.: Double sided cavity setup.

In the double sided external cavity setup shown in Figure 3.5.3.1, the light emitted from the laser diode is collimated by lenses on either side. On one side the beam is refracted by a grating and on the other side by a flat mirror. The output of this setup was taken off a beam splitter inserted into the beam path between laser and mirror. The beam splitter allowed a higher signal amplitude to the detector than the zero order reflection off the grating and prevented the circulating power in the cavity to saturate. The total cavity length was 25 cm while the spacing between the LD and the mirror was 13.8 cm.

3.6. LINEWIDTH AND MODE SPACING

Since laser linewidth and mode spacing measurements are an essential part of determining the quality of the alignment and therefore the coupling efficiency, various ways of determining an optical linewidth shall be explained here.

For standard SC laser diodes, a monochromator measurement is sufficient to resolve the modes of the Fabry-Perot cavity. The half meter scanning monochromator used has a reciprocal linear dispersion of 1.6 nm/mm. That is, with 100 μm slits at input and output a signal peak of FWHM (**F**ull **W**idth at **H**alf **M**aximum) = 1.6 Å can be resolved. With 50 μm slits a peak of FWHM = .8 Å and with 25 μm slits a peak of FWHM = .4 Å can be resolved. However, the monochromator has a resolution limit (limited by quality of optics and diffraction) of .07 nm FWHM or .7 Å. Hence, 50 μm slits give the best minimum resolution, since they allow more signal intensity to reach the detector and, at the same time, the resolution comes as close as possible to the resolution limit of the monochromator.

However, the mode spacing of the external cavity is expected to be much smaller than .8 Å, for example, 0.01321 Å for the 23.5 cm long cavity (see Table 3.6.1). The linewidth is even smaller than the mode spacing. Therefore other methods to determine them have to be found.

One of the possibilities is looking at the signal in the frequency domain. The 9 kHz to 1.8 GHz Tektronix Spectrum Analyzer 2712 has the frequency resolution necessary to detect two neighboring modes. A spectrum analyzer is basically a very narrow, tunable RF filter. This filter scans through the chosen frequency range and displays the detected signal components on an analog screen. The analyzer is able to detect two adjacent modes since frequency beating occurs between them.

Frequency beating is the phenomenon occurring when two modes of close frequencies ν_1 and ν_2 (or wavelengths) create a third mode of a frequency which corresponds to the difference $\Delta\nu$ of the two original modes or the "beat frequency". This is illustrated by the following equation for the total electric field of a signal with two modes:

$$E = E_1 + E_2 = |E_1| \cdot e^{j\omega 1 \cdot t} + |E_2| \cdot e^{j\omega 2 \cdot t}$$

with

$$e^{j\omega t} = \cos(\omega t) + j \sin(\omega t)$$

An optical detector responds to number of photons, hence, to the optical power, which is proportional to the square of the electric field:

$$E^2 = E \cdot E^* = |E_1|^2 + |E_2|^2 + 2\,|E_1| \cdot |E_2| \cdot \cos((\omega 1 - \omega 2) \cdot t)$$

where the difference in frequency (ω_2-ω_1) is called the beat frequency. Detecting this beat frequency will allow one to determine the mode spacing $\Delta\nu$ of the external cavity:

$$\Delta\nu = \frac{c}{2\,L\,n_{air}} \quad \text{or} \quad \Delta\lambda = \frac{\lambda_o^{\,2}}{2\,L\,n_{air}}$$

where L is the external cavity length, λ_o is the center frequency and n_{air} is the index of refraction of air. Thus, for the three external cavity lengths tested, the theoretical mode spacings are:

	L	$\Delta\lambda$	$\Delta\nu$
short cavity	8.2 cm	0.03786 Å	1.83 GHz
medium cavity	13.3 cm	0.02334 Å	1.13 GHz
long cavity	23.5 cm	0.01321 Å	0.64 GHz
standard laser diode	300 μm	2.8747 Å	143 GHz

Table 3.6.1.: External cavity lengths and corresponding mode spacings and mode spacing of standard laser diode.

One can see from table 3.6.1 that, compared to the standard laser diode, the external cavity modes will be spaced about a hundred times closer together. Figure 3.6.1 gives a qualitative picture of the diode mode spacing versus the external mode spacing.

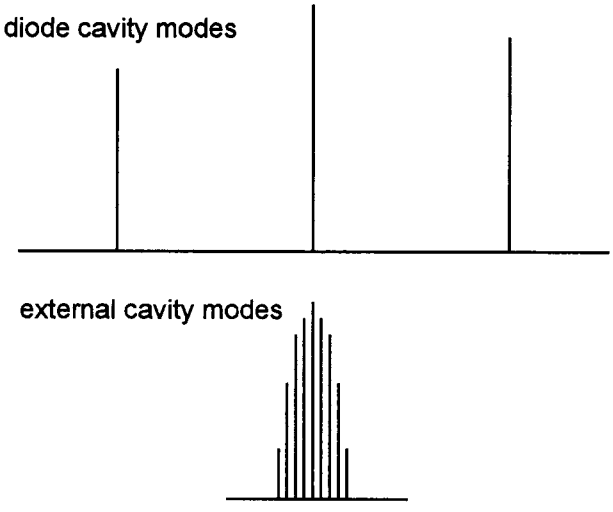

Figure 3.6.1.: Mode spacing of diode cavity and external cavity in comparison.

4. RESULTS AND DISCUSSION

In this chapter, the results of this thesis work are presented and discussed. Drive current vs. drive voltage or I-V-curves, optical power vs. drive current or P-I-curves and the wavelength spectra are given and explained. Finally, the results from the external cavity configurations are provided. The chapter closes with a short summary of all commercial laser diodes used here and their properties.

4.1. CHARACTERISTICS OF THE DIODES

All of the commercial diode lasers used showed typical I-V-curves following the equation:

$$I = I_o \left(e^{\frac{qV}{kT}} - 1 \right) .$$

All I-V-curves were taken with a Hewlett Packard Semiconductor Parameter Analyzer 4145B connected to a probe station with a Bausch & Lomb microscope. As an example, the curve of LD 14, a Mitsubishi ML4404 LD, is shown in Figure 4.1.1, where the horizontal ending of the curve is caused by the protective current limit which was set to 100 mA drive current. The current limit is set in order to prevent overdriving and damaging the diode.

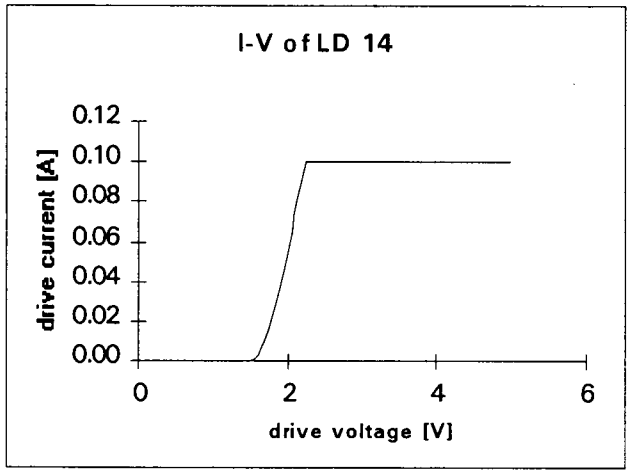

Figure 4.1.1.: I-V curve of LD 14, a Mitsubishi diode, with current limit of 100 mA.

The series resistance can be taken from the plot as a tangent to the linear region, i.e. at high voltage, where the series resistance dominates the total resistance.

$$R_{total} = R_{series} + R_{diode} \quad \text{where} \quad R_{diode} = \frac{kT/q}{I_{drive}}$$

As can be seen from the above equation, at small drive voltages and therefore small drive currents, the diode resistance is large and dominates the total resistance. The cut-on voltage, that is, the voltage at which the tangent to the rising drive current intersects with the voltage axis, stayed the same for all diodes, they all had a cut-on of 1.6 (±0.05) Volts.

While most diodes had identical I-V-characteristics, their spectral behavior or modal structure, changed considerably from diode to diode. Some diodes had smooth envelopes of the mode peaks below threshold, other diodes showed a more irregular envelope resulting from the fact that every third or fourth mode was unproportionally low in intensity. The repetition of the low intensity modes was not periodic, but rather random.

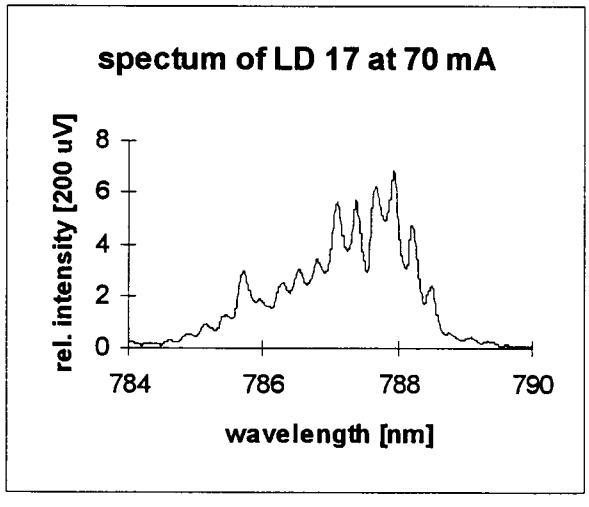

Figure 4.1.2.: Spectrum of LD 17 at a drive current of 70 mA.

Above threshold only some diodes stayed in a single mode operation. Lower quality diodes had several side modes or even supported two or more main modes until well

above threshold. An example is LD 17, a Sharp LT022MC laser, with spectral output shown in Figure 4.1.2 at a drive current of 70 mA. According to the manufacturer's specification, 70 mA was well above threshold. However, the laser is definitely not in single mode operation. One possible reason for the irregular spectra is the fact that many lasers were purchased at very low cost from a discount supplier, which means they may not have met manufacturing specifications and were therefore sold off at a lower price. Some of the LDs were used before they entered this project and might have been slightly degraded from that. A definite difference was visible between the cheaper and the more expensive versions. The change in their modal structure also affected their light emission curves or P-I-curves.

4.2. P-I-CURVES BEFORE AND AFTER COATING

As seen in earlier sections about AR coatings, the threshold of a laser diode shifts with the thickness and thus effectiveness of the coating. The exact equations and numerical results will follow later in this part. All P-I-curves were taken with the diodes mounted in an aluminum heat sink and pointing at a Newport Digital Power Meter, Model 815 with a calibrated attenuating filter. The beam was focused onto the detector with a collimating lens. Figure 4.2.1 shows the P-I-curve for the same laser diode LD 7 (Sharp LT023HC0, 785 nm) before (left) and after (right) applying a SiO AR coating to the output facet of the laser after removing the cap. The lasing threshold shifted from 46.5 mA with no coating to a drive current of 64 mA after coating one facet with a thin film of 1201 Å (and later to 84 mA after coating the second side). This is a measure for how well the AR coating reduced cavity feedback to the laser, since the drive current has to "drive" the gain higher to make up for the increased cavity losses through the facets. For example, an uncoated diode facet with a reflectivity of 31 % "loses" (transmits) 69 % of the incident power, while an AR coated diode facet with a residual reflectivity of 2 % "loses" 98 % of its power. The diode gain has to be increased far enough to exceed this loss in order to once again reach lasing threshold.

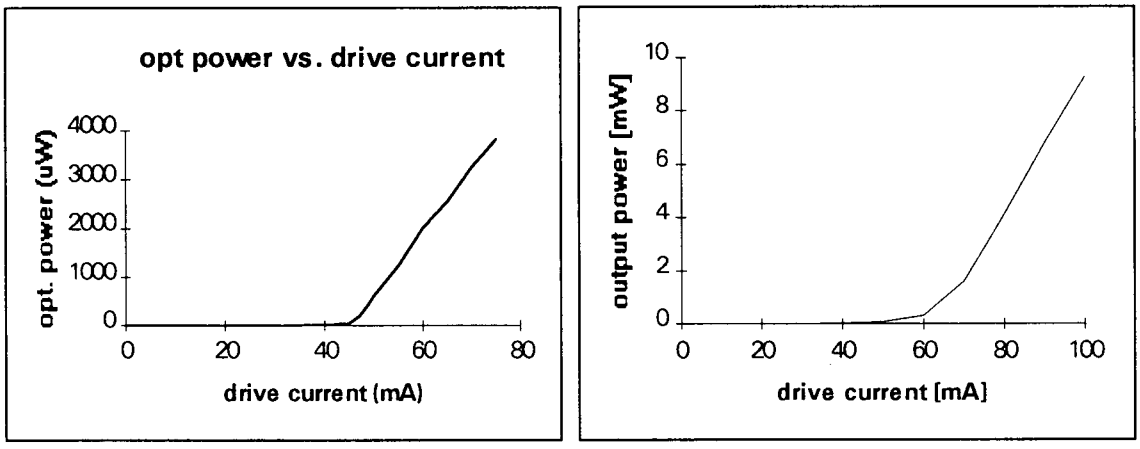

Figure 4.2.1.: Optical power output from one laser facet of LD 7 before AR coating depositions (left) and after AR coating deposition on one side (right).

The laser diode was then remounted on the previously described headers, wirebonded and coated on the second output facet. The P-I-curve after the second coating of LD 7 is shown in Figure 4.2.2.

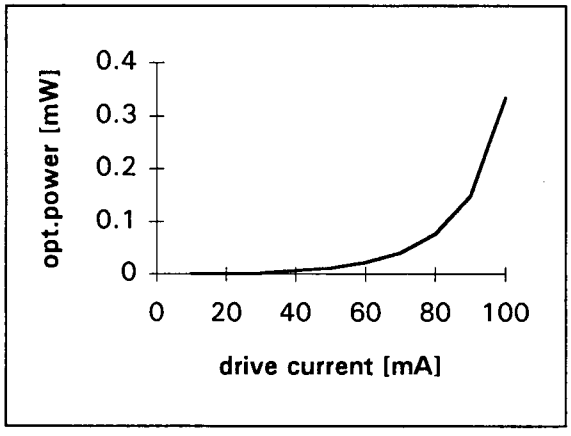

Figure 4.2.2.: Optical power output from one laser facet of LD 7 after AR coating deposition on both facets.

With the equations from section 2.2, the reflectivity can be calculated from the thickness of the coating and the refractive index, both determined from a reference film on a silicon wafer with an ellipsometer at the HeNe laser wavelength of 632.8 nm.

For LD 7 the thickness was 1065 Å and the index of refraction was 1.91 at 632.8 nm. Due to dispersion effects, the index at 788 nm will be slightly smaller. This results in a reflectivity of the first facet R'_1 of .19 %. The threshold current shifted from 46.5 mA to 57 mA, which according to the compensated equation by Ukita corresponds to a reflectivity R''_1 of 11.57%.

Or for LD 6 (Sharp LT023HC0, 788 nm) the thickness was 1073 Å and the index of refraction was 1.886. This results in a reflectivity of the first facet R'_1 of .09 %. The threshold current shifted from 45 mA to 50 mA, which according to the compensated equation by Ukita corresponds to a reflectivity R''_1 of 20.94%.

The large discrepancy in the calculated reflectivities has several reasons: For one, the reference thickness and index are measured next to the diode (the reference slab is positioned next to the diode during evaporation). This means that the actual thickness and index might be slightly different. A small thickness change, however, can result in a large

threshold current deviation. Secondly, the diode does not have an infinitely small spot size as is assumed for the ideal coating design. Therefore thickness and index for a perfect coating deviated a little. A third reason is that Ukita's equation is an empirical one and even in his own paper, the measurements do not exactly lay on his theoretical curve. The true reflectivity is somewhere in between R' and R''. For the coatings on the second side, the theoretical reflectivities R2 are .56 % and .21 % for LD 7 and 6, respectively. Ukita's equation does not apply for coatings of the second diode side.

Comparing all diodes, LD 9 (Sharp LT021MD0, 787 nm) had the best AR coating with a threshold current shift from 42 mA to 72 mA. A possible correlation between evaporation vacuum and coating quality was noticed. While the earliest as well as the most recent evaporations were performed at a pressure on the order of 10^{-7} Torr and produced good AR coatings, the evaporations in-between were made at a pressure of 10^{-6} Torr due to a small vacuum leak. These coatings increased the threshold currents less than the good coatings did. A poorer vacuum might result in a change of film density or stoichiometry which would affect its index.

The threshold current shift has been simulated in MATLAB using the reflectivity equations from chapter 2.2 as well as the following equation for diode laser threshold current which can be derived from Bhattacharya[32]:

$$I_{TH} = A \cdot J_{TH} = A \cdot \frac{8\pi\, q\, d\, \Delta\nu}{\eta_i\, \lambda^2\, \Gamma} \cdot \left(\alpha_i + \frac{1}{2L} \cdot \log(R_1 R_2)^{-1} \right)$$

where

A is the laser area,

d is the active layer thickness,

$\Delta\nu$ is the free spectral range,

η_i is the internal quantum efficiency,

λ is the center wavelength,

Γ is the confinement factor,

α_i is the internal loss,

L is the cavity length of the SC diode,

R_1 and R_2 are the reflectivities of the two facets.

See Appendix 1 for MATLAB scripts and plots of the program "single_side_coating.m".

This simulation "single_side_coating.m" shows how high the threshold current should rise depending on the coating thickness. The measured coating thickness and the corresponding threshold current after coating are shown for LD 1 (Sharp LT021MC0, 788 nm), 2 (Sharp LT021MC0, 788 nm) and 3 (Sharp LT027MD0, 788 nm) with little x-marks in the graph.

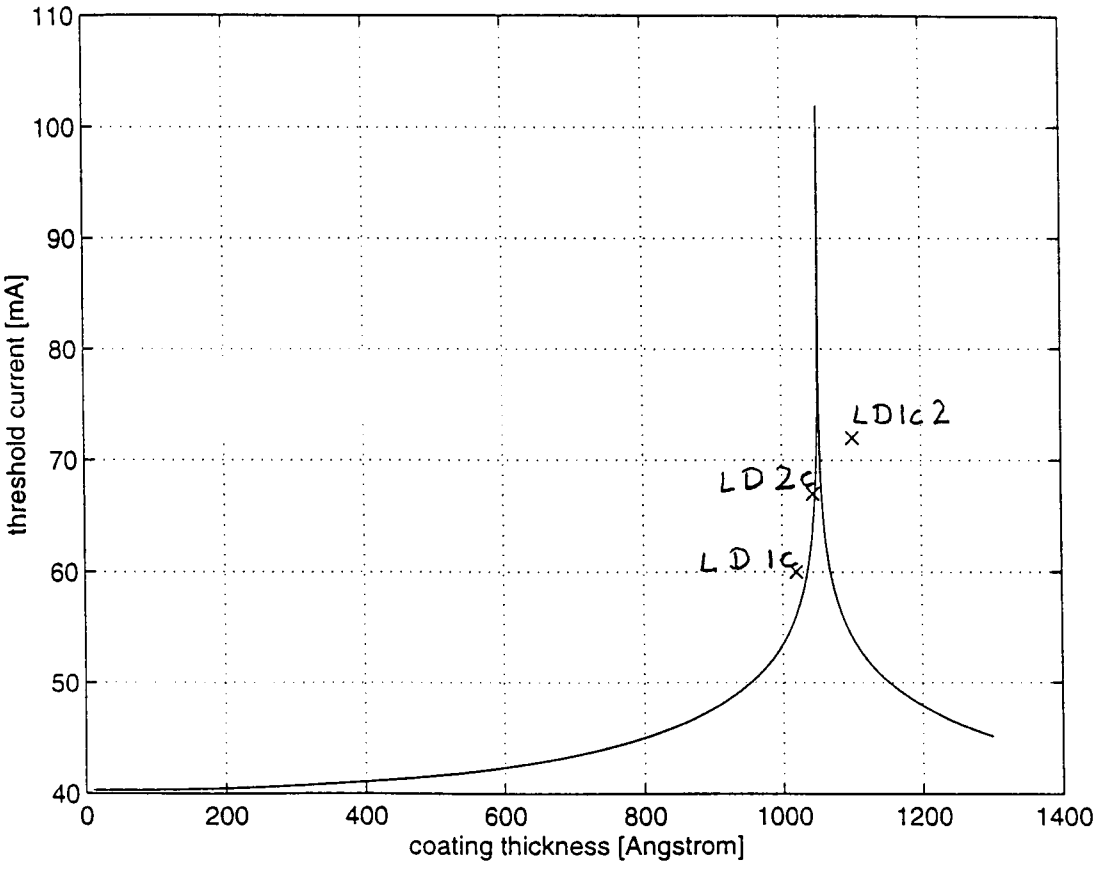

Figure 4.2.3.: Output of the MATLAB program "single_side_coating.m".

4.3. MONOCHROMATOR SPECTRA

The monochromator spectra were obtained using the setup shown in Figure 4.3.1 using a Chromex 500 SM Scanning Monochromator with control module attachment and a 1180 grooves/mm, 500 nm blaze wavelength grating to tune through the wavelength range. The detector is a fast (< 1 ns) silicon PIN photodiode from Thorlabs. Its output was fed into a current sensitive preamp (PAR Model 184) in a Princeton Applied Research lock-in-amplifier (Model 124 A), which is a current amplifier ranging from .2 Hz to 210 kHz. The data acquisition board transforms the lock-in-amplifier signal to a 0-10 V (actually -10 to 10V) output which is finally routed to the computer for data manipulation and plotting.

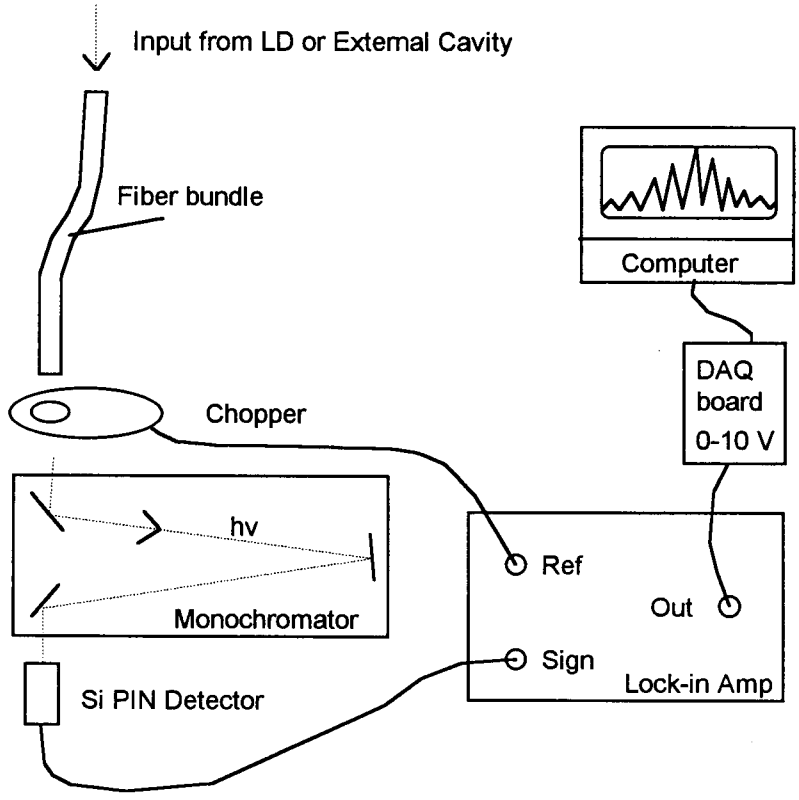

Figure 4.3.1.: Setup for acquiring the monochromator spectra of laser diodes or the external cavity output, respectively, involving a data acquisition (DAQ) board and a lock-in current amplifier.

The monochromator spectra of the coated and uncoated diodes looked similar when the AR coated diodes were driven above their higher threshold current value. The diode will still exhibit laser behavior since the remaining reflectivity of about 0.1 % - 5 % from the imperfect AR coatings provides loss which has to be compensated for by the gain inside the active material. As soon as the gain exceeds the mirror losses and distributed losses, the diode changes from the spontaneous to the stimulated regime. Figures 4.3.2 - 4.3.5 show typical monochromator spectra (here LD 7 after a second AR coating) at increasing drive currents from 60 mA to 90 mA and with intensity scales varying from 5 mV to 2000 mV.

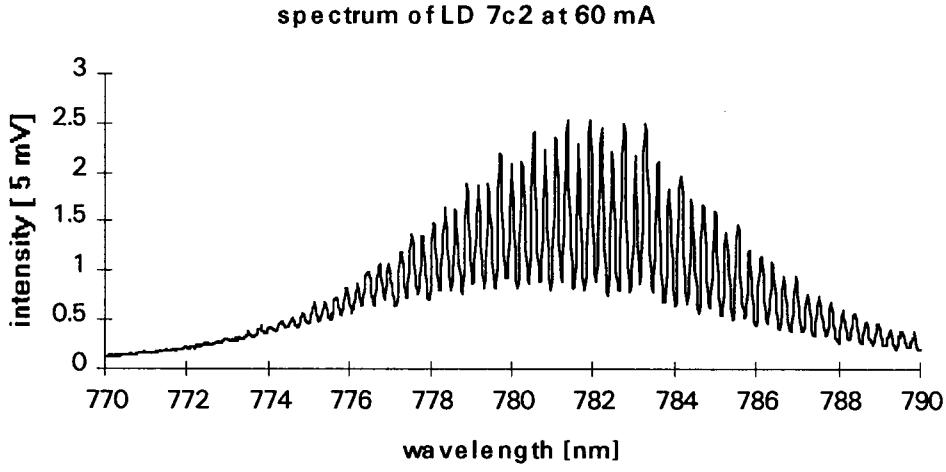

Figure 4.3.2.: Monochromator spectrum at 60 mA drive current and with an intensity scale of 5 mV.

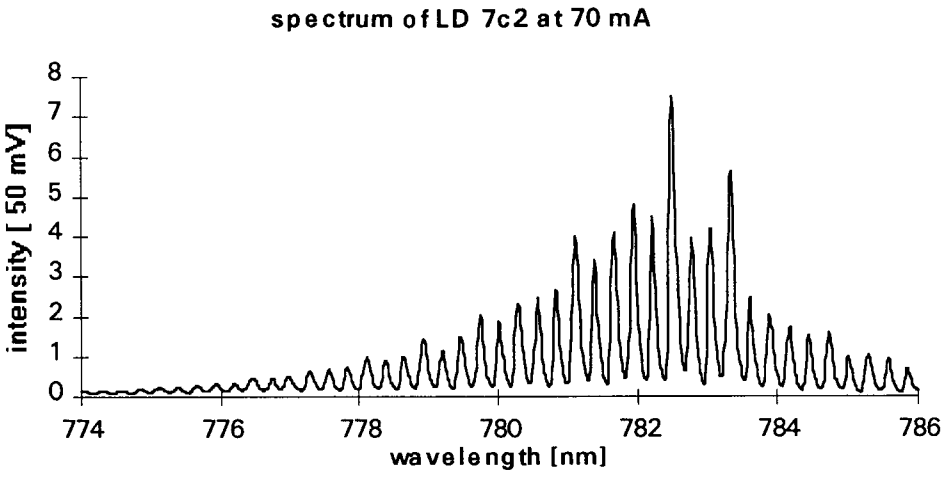

Figure 4.3.3.: Monochromator spectrum at 70 mA drive current and with an intensity scale of 50 mV.

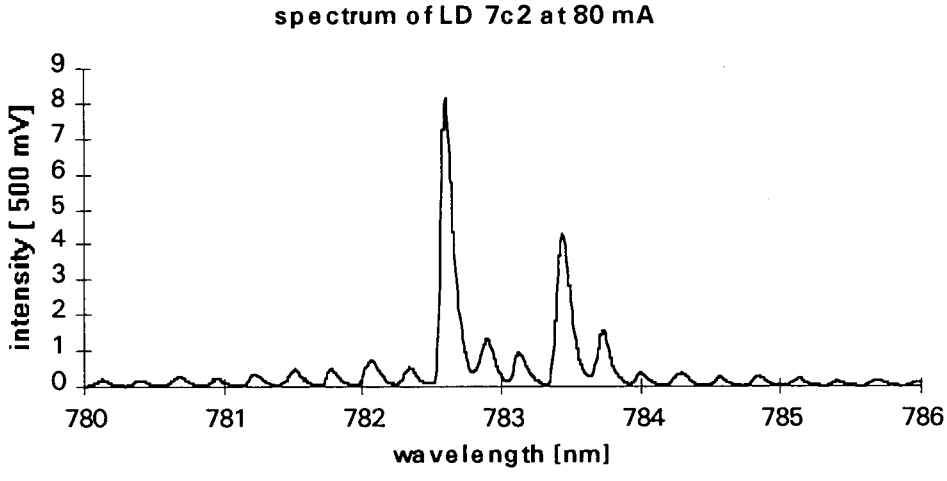

Figure 4.3.4.: Monochromator spectrum at 80 mA drive current and with an intensity scale of 500 mV.

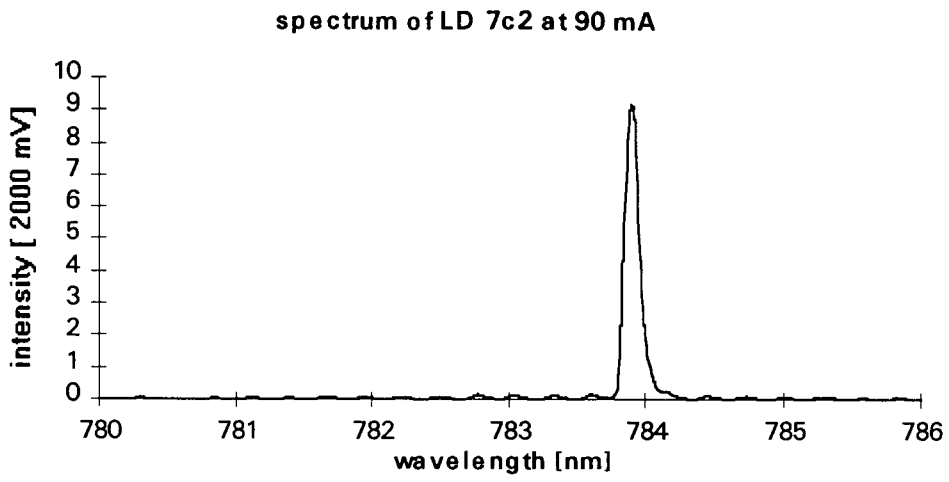

Figure 4.3.5.: Monochromator spectrum at 90 mA drive current and with an intensity scale of 2000 mV.

As mentioned earlier, the output of the lock-in-amplifier goes to a data acquisition board with maximum amplitude output of 10 (Volts). Thus, full scale of "10" on the y-axis corresponds to the intensity scale setting of the lock-in as noted on each figure.

4.4. EXTERNAL CAVITY OBSERVATIONS

To better distinguish between the different cases in this chapter, I will refer to an uncoated diode without external cavity as LD # and to a diode coated on one end without external feedback as LD #c. An uncoated diode in the external cavity will be referred to as EC #, and finally a diode coated on one end in the external cavity is EC #c. The numbers in the upcoming plots are date and number of measurement, e.g. 11-3-5 stands for the 5th measurement on November 3rd.

4.4.1. Single sided cavity with a grating output

This section will compare the spectra, tuning range and threshold behavior of LD 12 (a Sharp LT027MD0 commercial diode laser) in an external cavity before and after coating one facet. It will also take a closer look at the impact of the cavity length on the aforementioned properties. Three cavity lengths were used: 8.2 cm for the short cavity, 13.3 cm for the medium one and 23.5 cm for the long cavity. The odd numbers of the cavity lengths were a result of the size and tilt angle of the mounts in combination with the constant 1-inch spacing of the holes in the optical plate and table. Figure 4.4.1.1 shows measurements of LD 12 without external feedback and Figure 4.4.1.2 those of EC 12 in the medium length cavity.

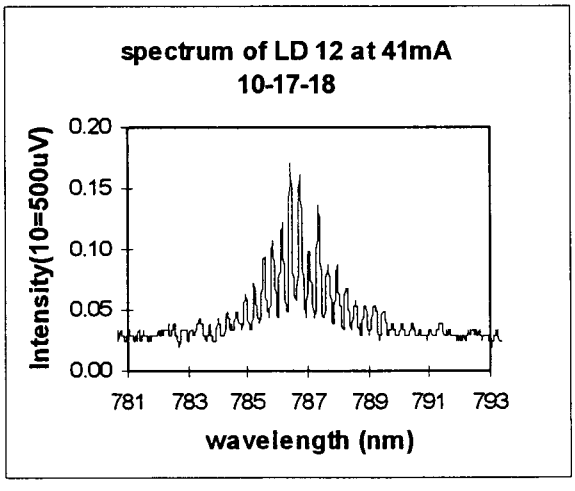

Figure 4.4.1.1.: Spectrum of LD 12 at 41 mA, i.e. at threshold, without external cavity.

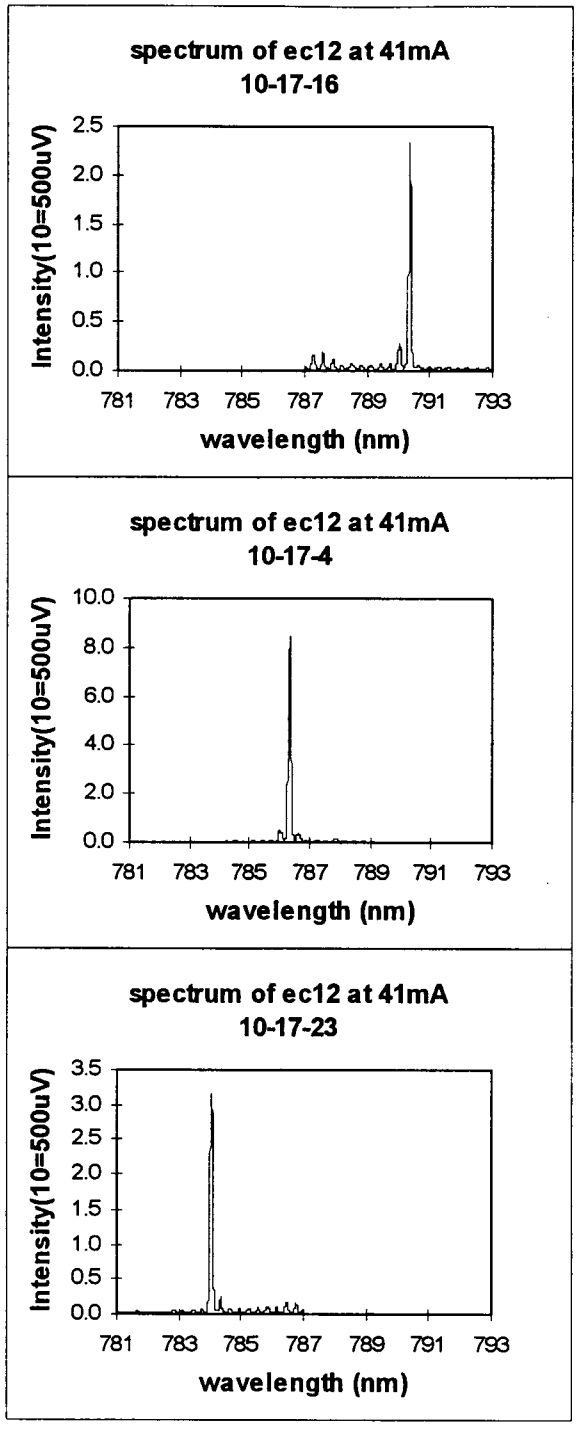

Figure 4.4.1.2.: Spectra of LD 12 at 41 mA in a medium external cavity (from top to bottom): tuning from 790.3 nm, over 786.6 nm, to 784 nm.

While earlier measurements were taken with the grating mounted on an inexpensive Daedal mirror mount with 8-32 Allen-head adjustment screws, the diode spectra in this section were obtained using a Newport MM-1 mirror mount with 80-pitch (80 threads/inch) adjustment screws, which allow extremely fine tuning. This was not possible with the original grating mounts.

The above plots of EC 12 show the main peak of the spectra tuning through a range of about 6.3 nm (784 nm to 790.3 nm) which was achieved by rotating the grating about its vertical axis. The angle of rotation change was always fractions of a degree (or μrad), which means a minimum of movement of the grating shifted the intensity peak several nanometers. Towards the edge of the tuning range, the intensity of the peaks became continually lower as expected from the gain curve.

The tuning range varied with the length of the cavity. The tuning range is defined by the difference between the shortest and the longest possible single mode to which the cavity can be tuned. While the medium cavity had the largest tuning range with 6.3 nm, the short cavity showed a tuning range of 1.8 nm. The power amplification factors of these measurements were 50 and 40, respectively. This indicates that the longer cavity gives a wider tuning range with the limitation that the power of the feedback decreases with distance due to dispersion losses.

Another set of measurements in the same setup with LD 19 proved the continuation of this trend with an even longer cavity of 23.5 cm. The short cavity with LD 19 had a tuning range of 3.2 nm, the medium cavity one of 4.2 nm and the long cavity rendered 8.4 nm.

After these measurements, the cap was removed from the LD package and an antireflection coating was applied to the output facet as described in chapter 3. LD 12 was now LD 12c. The thickness and index of refraction were determined by ellipsometry from a reference sample placed into the evaporation chamber with the diode.

The coating on the front facet of LD 12c increased the threshold from 40 mA to 60 mA drive current. The spectra of LD 12c without an external cavity displayed a much wider FWHM or "bandwidth" compared to the uncoated diode LD 12. At 40 mA and 60 mA the bandwidths of LD 12c were 18 nm and 8 nm (see Figure 4.4.1.3), respectively, where the reduced bandwidth at 60 mA is the result of gain-narrowing mechanisms. The corresponding bandwidths at the same drive currents of LD 12 before coating were 3.5 nm and 0.2 nm, respectively, where the 0.2 nm were the linewidth of a single mode. The increased bandwidth should provide a much wider tuning range when the AR coated diode is placed into the external cavity. And, in fact, for all three tested cavity lengths the tuning range did increase significantly using the AR coated diodes.

Figure 4.4.1.4 shows that the intensity peak of LD 12c in the long cavity shifted from 772 nm to 790 nm as the grating angle was changed. Thus, the single mode tuning range was 18 nm, which is remarkably wider than the FWHM of 8 nm of the standard diode.

The addition of the external cavity and the antireflection coating resulted in a broader tuning range and a narrower bandwidth compared to the standard uncoated diode.

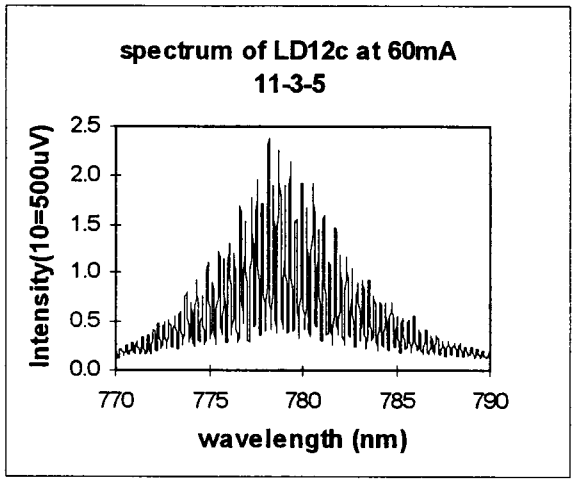

Figure 4.4.1.3.: Spectrum of LD 12c at 60 mA with a FWHM of 8 nm without external cavity.

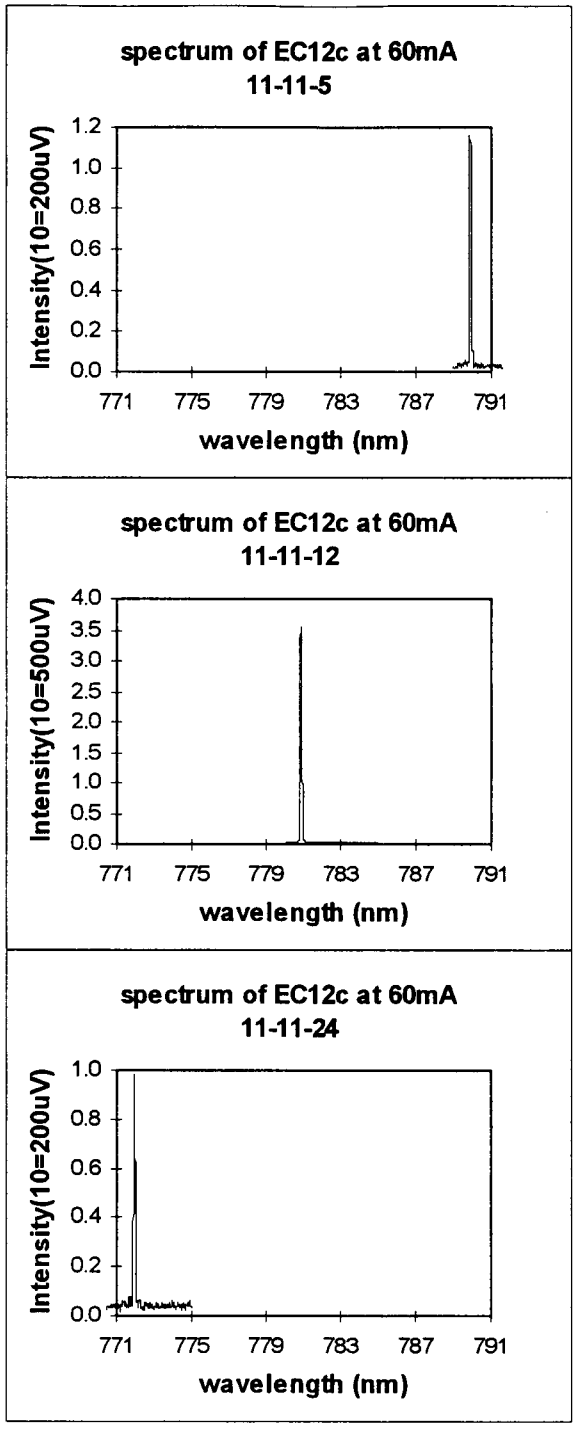

Figure 4.4.1.4.: Spectra of LD 12c in a long external cavity (from top to bottom): tuning from 790 nm, over 780.9 nm, to 772 nm.

The short and medium external cavities displayed tuning ranges of 8 nm and 10.3 nm, respectively. The power amplification factors of these measurements were 60 and 65, respectively. The power amplification factor is the power output of the aligned cavity vs. the power output of the unaligned cavity. With the long cavity, a power amplification of 50 was achieved. Again, the tuning range increased with larger cavity length.

In summary, the bandwidth of LD 12 increased after application of the AR coating from 3 to 18 nm at 40 mA and from .12 to 8 nm at 60 mA (see Table 4.4.1.1). The addition of an external cavity decreased the lasing linewidths of each device. The linewidths of the external cavities are very close to the resolution of the monochromator, which is given as .07 nm by the manufacturer. This indicates, that the actual linewidths of the external cavities might be even more narrow, if they could be measured with an instrument of finer resolution.

device	bandwidth at 40 mA	bandwidth at 60 mA
LD 12	3 nm	0.12 nm
EC 12	0.08 nm	not measured
LD 12c	18 nm	8 nm
EC 12c	not measurable	0.1 nm

Table 4.4.1.1.: Bandwidths of LD 12, EC 12, LD 12c and EC 12c.

The application of an AR coating also increased the tuning range of EC 12 or EC 12c from 6.3 nm to 10.3 nm. For all cavities the tuning range increased with cavity length. See also Table 4.4.1.2.

cavity length	tuning range of EC 12	tuning range of EC 19	tuning range of EC 12c
8.2 cm	1.8 nm	3.2 nm	8 nm
13.3 cm	6.3 nm	4.2 nm	10.3 nm
23.5 cm		8.4 nm	18 nm

Table 4.4.1.2.: Tuning ranges of LD 12, EC 12, LD 12c and EC 12c.

Another set of measurements was taken to examine whether the external cavity stabilizes the lasing wavelength of the SC laser over a wide range of drive currents. The cavity was tuned to a set wavelength and then the drive current was increased incrementally from 55 mA to 100 mA. It turns out that the cavity stabilizes the wavelength quite well. For the laser with an external cavity the fluctuation of the main peak was smaller than .3 nm over a variation of 45 mA in the drive current. The actual variation may even be smaller, since the resolution of the monochromator is close to this fluctuation range and thermal variations in the room from the air-conditioning system could not be avoided. Without the external cavity, the center frequency of the laser moved about 2.2 nm over a similar drive current range. This property of high stability could increase the number of signals that can be sent through a fiber optic cable using wavelength division multiplexing since it reduces the spacing which must safely separate two signal wavelengths to insure that they do not overlap.

It has been explained in chapter 2 why diode lasers normally change their center wavelength. Heating effects change the index of refraction of the active material, the diode length, and the band gap E_G of the active material while harder pumping shifts the gain curve. The above experiments have demonstrated a method to counteract these phenomena and stabilize the center wavelength.

As expected from theoretical considerations, the threshold current of the diode in a cavity is lower than the threshold current of the coated diode without cavity. In the case of LD 12c, the threshold decreased from 60 mA without a cavity to 50 mA in the cavity. This phenomenon is caused by the increased feedback from the grating lowering the loss and causing the threshold condition of "gain equals loss" to occur at a lower drive current. This is visualized in Figure 4.4.1.5. Theoretically, the threshold should be lower than the

initial one since the feedback from the grating is higher than from the original uncoated diode facet. However, diffraction losses from propagation, as well as diffraction and loss at the lens can raise the loss line and therefore raise the threshold current.

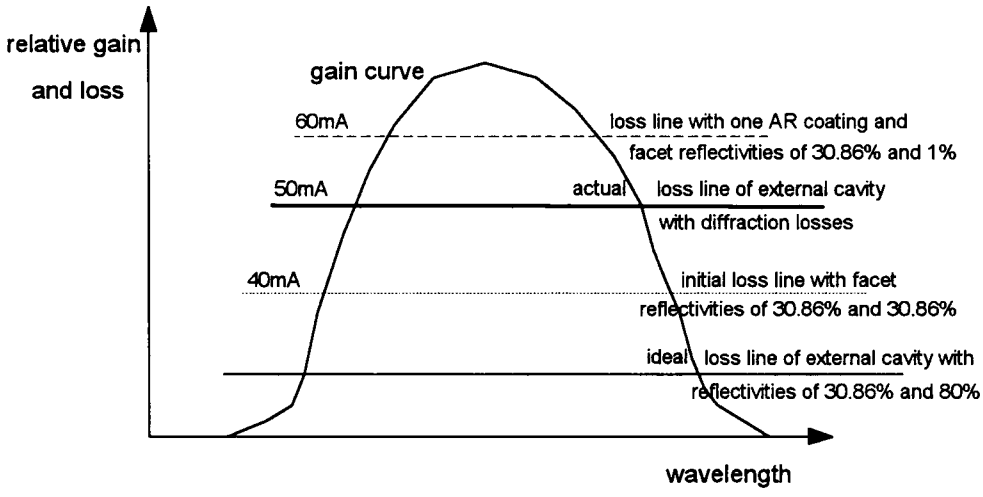

Figure 4.4.1.5.: Relative gain and loss lines describing threshold condition of "gain equals loss" for the uncoated diode LD 12, single-side-coated diode and in the external cavity. The corresponding measured threshold currents are noted on the left hand side.

The external cavity spectra for the uncoated and coated diode were taken at different drive current levels. This is because the diode needs to be close to the threshold in order to provide enough output to obtain a single mode by means of feedback. In the case of LD 12c, this means that even if the light was coupled back into the cavity at 40 mA, one might not be able to see one clear single mode and then determine tuning ranges or center frequencies. As mentioned previously, the variation of the peak wavelength with drive current in an external cavity configuration is very small. Therefore, all tests were performed at the threshold of the specific diode in order to ease the identification of an uncoupled versus a coupled cavity.

All test were also performed on an optical breadboard base made from aluminum, which was fabricated to provide stability for the optical components. It also makes the cavity an easily transportable system.

4.4.2. Double sided cavity with mirror and grating

With the spectral measurement setup mentioned previously in this chapter, the following external cavity spectra of LD 4 (Sharp LT023HC0, 787 nm) were measured. LD 4 was coated on both sides at the time of the experiment. The external cavity configuration can be seen in Figure 3.6.3.1. The spectra show a shift of the center wavelength to longer wavelength with increasing drive current, that is, with increasing gain. This is mainly due to heating effects, since the diodes were driven in a continuous mode. Heating can be reduced by pulsed operation or cooling with Peltier elements.

We can see that the frequency spacing of adjacent modes is approximately 3 Angstroms or .3 nm which is close to the calculated mode spacing of 2.8747 Å (see chapter 3) and corresponds to:

$$\Delta\nu = \frac{c}{2nL} \quad \text{or} \quad \Delta\lambda = -\frac{c}{\nu^2}\,\Delta\nu = -\frac{\lambda_o^{\,2}}{c}\frac{c}{2nL} = -\frac{\lambda_o^{\,2}}{2nL}$$

for a cavity length L of approximately 300 μm, the length of the semiconductor cavity, and an index of refraction of 3.6. Those residual oscillations occur because of deviations in the coating thicknesses and indices of refraction which result in a non-zero reflection coefficient of the facets. However, they are strongly reduced compared to the initial uncoated cavity, where the side modes have a much greater influence.

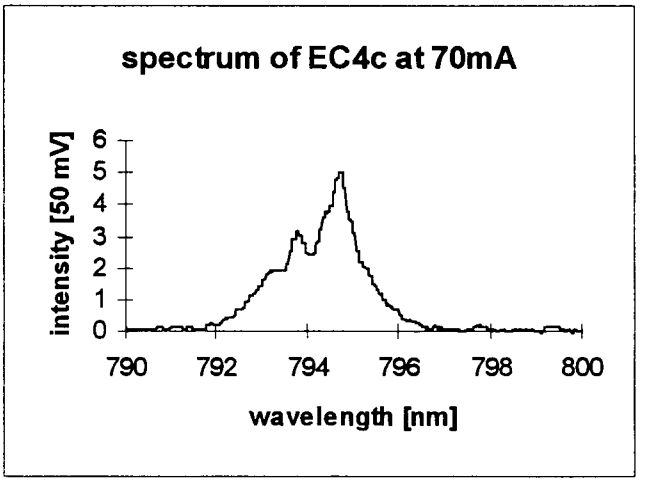

Figure 4.4.2.1.: Monochromator spectrum of external cavity with laser diode #4 at I_D=70 mA.

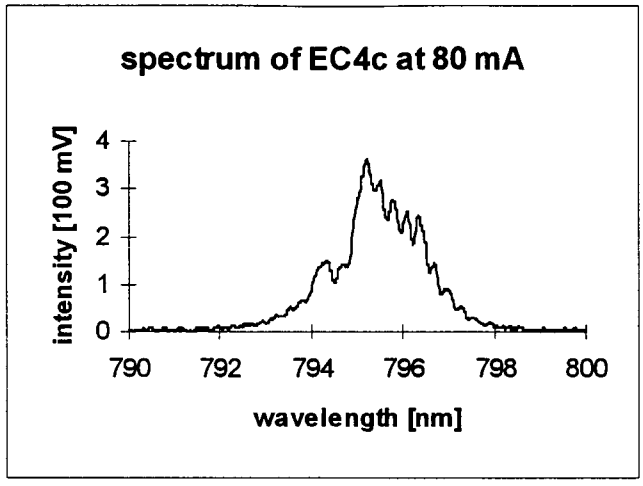

Figure 4.4.2.2.: Monochromator spectrum of external cavity with laser diode #4 at I_D=80 mA.

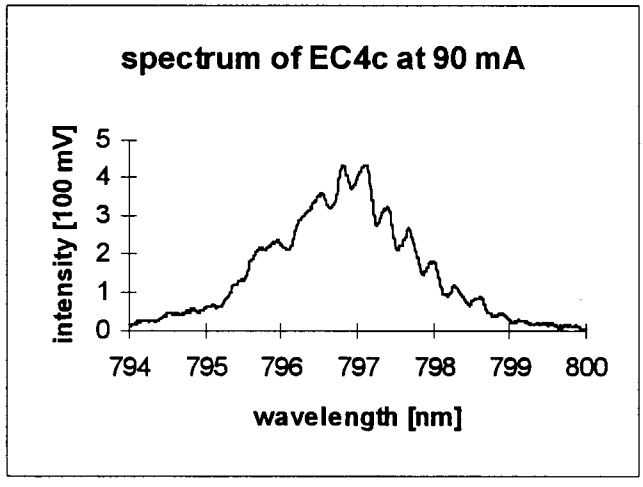

Figure 4.4.2.3.: Monochromator spectrum of external cavity with laser diode #4 at I_D=90 mA.

The power amplification of the external cavity was measured by relating the output of the diode laser without feedback and the output of the external cavity and is displayed in Figure 4.4.2.4. The power amplification factor is related to the coupling coefficient,

which is the ratio of light that gets coupled back into the active region (and there amplified again). The length of the cavity was 25 cm.

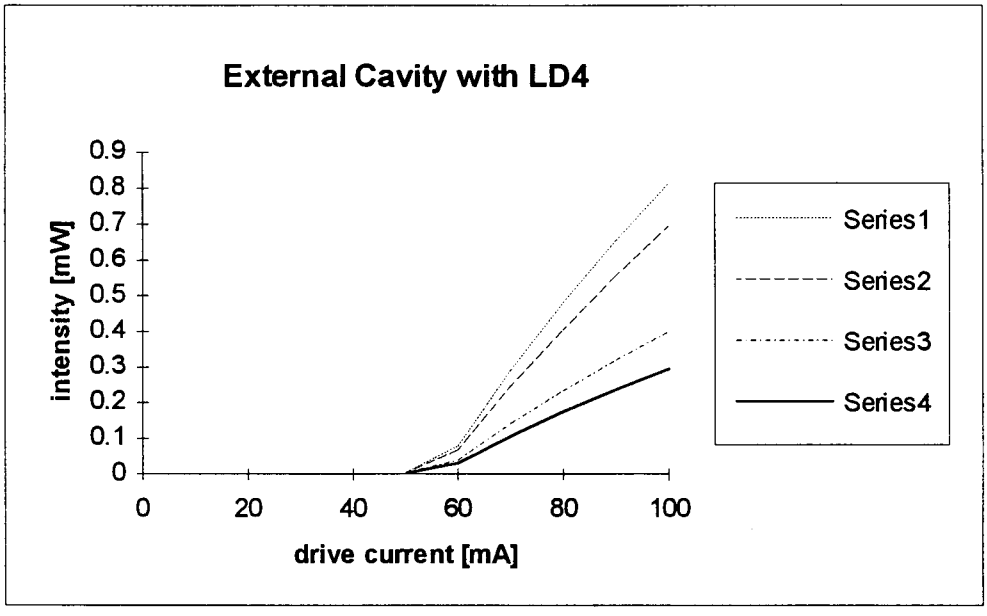

Figure 4.4.2.4.: P-I-curve of external cavity output of laser diode #4 with mirror and grating (Series 1), with mirror feedback only (Series 2), with grating feedback only (Series 3), without any feedback (Series 4).

The power amplification factor of this case was 2.7466. In later, improved setups it went as high as 4.3529 for the double sided cavity.

4.5. DIODE LASER INFORMATION

This section is a collection of significant data concerning the diodes used for this project as well as of the material constants and related information. The purpose of this chapter is more to provide a structured section to look up supporting information and give an overview, rather than to explain.

The commercial diodes were manufactured by Sharp and Mitsubishi and had the following data (with slight deviations in the wavelength):

free space wavelength:	$\lambda_0 = 788$ nm
energy gap: [11]	$E_G = 1.5736$ eV $= (1.424 + 1.247x)$ eV for $0 < x < 0.45$
aluminum concentration:	$x = 12\%$
index of active layer material:[33]	$n(x) = 3.59 - 0.71x + 0.091\,x^2 = 3.5061$
lattice constant:[34]	5.65 Å
	Note: close lattice matching of AlAs and GaAs results in low threshold currents and low temperature sensitivity, which are desirable features of a laser diode.
attenuation constant of active layer:	10-15 1/cm [35], 150-200 1/cm [36]
typical threshold currents:	500A/cm^2
typical gain coefficient:	4.5 10^6 cm^2/A
assuming plane wave incidence:	
ideal film index:	$n_F = (n_{AlGaAs})^{1/2} = 1.8725$
ideal film thickness:	$l = \lambda/4 = \lambda_0/4\,n_F = 1052$ Å

typical diode dimensions:

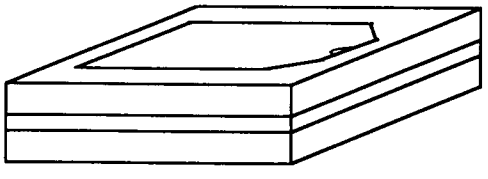

length L = 300 μm
stripe width s (buried V groove) = 10 μm
active layer thickness d = 1000 Å

Figure 4.5.1.: Close-up view of a Sharp laser diode.

reflectivity R_o before AR coating:

$$R_o = \frac{(n_{substr} - n_{air})^2}{(n_{substr} + n_{air})^2} = \frac{(3.5-1)^2}{(3.5+1)^2} = 30.86\%$$

device	model #	center wavelength	threshold current
diode 1	Sharp LT021MC0	788 nm	39.4 mA
diode 2	Sharp LT021MC0	788 nm	38.5 mA
diode 3	Sharp LT027MD0	788 nm	40.9 mA
diode 4	Sharp LT023HC0	787 nm	45.9 mA
diode 5	Sharp LT023HC0	788 nm	49.2 mA
diode 6	Sharp LT023HC0	788 nm	46.7 mA
diode 7	Sharp LT023HC0	785 nm	46.5 mA
diode 8	Sharp LT023HC0	785 nm	48.2 mA
diode 9	Sharp LT021MD0	787 nm	42.5 mA
diode 10	Sharp LT021MD0	789 nm	42.8 mA
diode 11	Sharp LT027MD0	788 nm	35.0 mA
diode 12	Sharp LT027MD0	788 nm	40.2 mA
diode 13	Mitsubishi ML4404	773 nm	37 mA
diode 14	Mitsubishi ML4404	774 nm	42 mA
diode 15	Mitsubishi ML4404	772 nm	43 mA
diode 16	Sharp LT022MC	788 nm	45 mA
diode 17	Sharp LT022MC	789 nm	50 mA
diode 18	Sharp LT022MC	788 nm	40 mA
diode 19	Sharp LT031MD0	750 nm	38 mA

Table 4.5.1.: List of laser diodes used in this project, their threshold currents and center wavelengths.

5. CONCLUSIONS AND SUGGESTIONS FOR FUTURE WORK

The goal of this project was to build an external cavity laser diode and to investigate the effects of the external cavity on typical laser properties, such as threshold current, optical power output, spectral behavior, bandwidth, tuning range, wavelength stability with varying drive current and mode spacing.

The commercial diode lasers used operated in the infrared wavelength range with a nominal wavelength of 788 nm. The active medium consisted of AlGaAs. The external cavity provided high stability through optical feedback.

To reduce parasitic oscillations from the diode cavity an antireflection of 1052 Å thick SiO AR coating was applied onto both sides of the diode. The AR coatings sufficiently reduced the SC-air reflection coefficient to explore the behavior of the external cavity. The achieved reflectivities calculated from the coating thicknesses and indices range between .69 % for LD 12 and .09 % for LD 6. The threshold currents shifted between 5 mA for LD 6 and 30 mA for LD 9. The reflectivities calculated from the shift in threshold current were 20.94 % (LD 6) down to 2.1 % (LD 9). The discrepancies reflect the difficulties in measuring the exact thickness and index of the coating as well as the lack of control over the film density during evaporation.

The diodes were tested, antireflection coated and then re-examined in the cavities. The external cavity clearly showed an additional power gain compared to the AR coated diode without external feedback. In most cases, the power output of the external cavity with feedback was about 50 times higher than the power from the setups without feedback.

The tuning ranges increased after the deposition of the AR coating from 1.8 nm to 8 nm for a cavity of 8.2 cm length and from 6.3 nm to 10.3 nm for a cavity of 13.3 cm length. The gain bandwidth of each laser was increased by means of the AR coating. For LD 12 it increased from 3 to 18 nm.

A more stable mount and more precise adjustment were necessary to research other features like mode selectivity and lower threshold. The mode selectivity appeared to be excellent with 80-pitch adjustment screws. Wide tuning ranges have been obtained with this kind of precise alignment and focusing. By means of the grating, the resonating wavelength of the external FP cavity could be adjusted by up to 18 nm in single mode operation. The lowering of the threshold from 60 mA to 50 mA by means of the external

cavity has been shown, however a reduced dispersion loss seems desirable to even decrease the threshold further.

Also, the tuning range was shown to increase with the cavity length. For the uncoated LD 19 the tuning range increased from 3.2 m to 4.2 nm to 8.4 nm in a 8.2 cm, a 13.3 cm and a 23.5 cm long external cavity, respectively. The coated laser 12 was tunable over 8 nm, 10.3 nm and 18 nm in the above named cavity lengths. The largest tuning range was obtained with the coated diode laser in the large external cavity of 23.5 cm length.

The external cavity with an AR coated diode laser was shown to have improved wavelength stability with increasing drive current compared to a standard laser diode without an external cavity. Instead of a wavelength shift of 2.2 nm over 45 mA difference in drive current for the free laser, the external cavity output wavelength only shifted by 0.3 nm over the difference in drive current.

Possible work on this project in the future may involve packaging the whole assembly into a rugged, "student-proof" unit, temperature control of the laser diode mount and also documentation, such that it can be used by students in the two optoelectronics classes.

A better semiconductor material with quantum well design needs to be fabricated, since the material used in this project showed a high series resistance making it unfit for further use. Longer diode stripes need to be grown to provide more gain for use in SC laser noise measurement at UofO. The tilted angle processing needs to be implemented on these structures.

Also, a diode array detector for use on the monochromator would be extremely helpful for real-time spectral measurement ease.

Additional work needs to be done measuring the noise spectrum, linewidth of the external cavity, stability and lifetime of the AR coated gain material.

Possible applications for the external cavity are mentioned in chapters 1 and 2. This external cavity diode laser will be used in the Optoelectronics Lab for further research. For example, with a 15 cm cavity length and a 500 MHz pulsed or sinusoidal drive current, it might be possible to mode-lock the laser for picosecond pulse generation. Secondly, it might be used for Rubidium research and OTDR checking.

This project designed, fabricated and measured the behavior of external cavity diode lasers using commercially available semiconductor lasers. Antireflection coatings

were designed and applied successfully to the laser facets. New headers were designed and built and techniques were successfully developed to remove the laser diodes from their commercial packages and remount them onto our own headers with little degradation in performance. The external cavity diode lasers were shown to have the benefits of a broad, single-mode tuning range, narrow linewidth and improved wavelength stability. The effects of the addition of AR coatings and of varying the cavity length on the performance of the laser were studied and quantified. Several problems occurred during the project, such as varying AR coating thicknesses and quality and high series resistance in the initial active material grown at OSU; however, each one lead to better insight and understanding. This external cavity laser will be used to probe the fundamental noise properties of SC laser gain media.

BIBLIOGRAPHY

[1] Y. Hori, H. Asakura, F. Sogawa, M. Kato, H. Serizawa, "External-cavity semiconductor laser with focusing grating mirror", IEEE J. Quantum Electron., vol. 26, no. 10, pp. 1747-1755, 1990.

[2] J. McInerney, L. Reekie, D. J. Bradley, "Observation of bistable optical effects in a twin GaAs/GaAlAs diode external cavity ring laser", Electron. Lett., vol. 20, no. 14, pp. 586-588, 1984.

[3] S. Norimatsu, K. Iwashita, K. Noguchi, "An 8 Gb/s QPSK optical homodyne detection experiment using external-cavity laser diodes", IEEE Photon. Lett., vol. 4, no. 7, pp. 765-767, 1992.

[4] B. E. A. Saleh, M. C. Teich, "Fundamentals of photonics", John Wiley & Sons Inc., New York, 1991.

[5] A. K. Datta, A. Paul, G. S. Sanyal, "Study of the variation of refractive index and material dispersion with wavelength from attenuation data", J. of Appl. Physics, vol. 56, no. 7, pp. 1965-1968, 1984

[6] W. F. Sharfin, A. Mooradian, C. M. Harding, R. G. Waters, " Lateral-mode selectivity in external-cavity diode lasers with residual facet reflectivity", IEEE J. Quantum Electron., vol. 26, no. 10, pp. 1756-1763, 1990.

[7] P. Klocek, Handbook of infrared optical materials, "Optical thin-film coatings", Marcel Dekker Inc., New York, pp. 483-497, 1991.

[8] I. Ladany, P. J. Zanzucchi, J. T. Andrews, "Scandium oxide antireflection coatings for superluminescent LEDs", Appl. Optics, vol. 25, no. 4, pp. 472-473, 1986.

[9] G. Eisenstein, L. W. Stulz, "High quality antireflection coatings on laser facets by sputtered silicon nitride", Appl. Optics, vol. 23, no. 1, pp. 161-164, 1984.

[10] S. Ramo, J. R. Whinnery, T. van Duzer, "Fields and waves in communication electronics", John Wiley & Sons Inc., New York, pp. 285-299, 1984.

[11] H. C. Casey, M. B. Panish, Quantum Electronics/Principles and Applications, "Heterostructure Lasers", part B: "Materials and Operating Characteristics", p. 16, table 5.3-1, 1978.

[12] P.-H. S. Yeh, I.-F. Wu, S. Jiang, M. Dagenais, "35-dB Small-Signal-Gain High-Power Diffraction-Limited Tapered Semiconductor Amplifier", LEOS conference, pp. 588-9, 1990.

[13] S. C. Sahyun, "Mode Transitions of an External Cavity Diode Laser", Thesis of Master of Science in Physics, Montana State University, p. 13, 1992.

[14] P. B. Hansen, G. Raybon, U. Koren, "In GaAsP monolithic extended-cavity lasers with integrated saturable absorbers for active, passive and hybrid mode locking at 8.6 GHz", Appl. Physics Lett., vol. 62, no. 13, 1993.

[15] M. Schell, A. G. Weber, E. H. Böttcher, E. Schöll, D. Bimberg, "Theory of subpicosecond pulse generation by active mode-locking of a semiconductor laser amplifier in an external cavity: limits for the pulsewidth", IEEE Photon. Technol. Lett., vol. 27, no. 3, pp. 402-409, 1991.

[16] R. F. Broom, E. Mohn, C. Risch, R. Salathe, "Microwave self-modulation of a diode laser coupled to an external cavity", IEEE J. of Quantum Electron., vol. 6, no. 6, 1970.

[17] J. M. Hammer, "Closed form theory of multicavity reflectors and the output of external diode lasers", IEEE J. of Quantum Electron., vol. 20, no. 11, pp. 1252-1259, 1984.

[18] D.-S. Seo, J.-D. Park, J. G. McInerney, M. Osinski, "Multiple feedback effects in asymmetric external cavity semiconductor lasers", IEEE J. of Quantum Electron., vol. 25., no. 11, pp. 2229-2237, 1989.

[19] N. K. Dutta, N. A. Olsson, "Effect of external optical feedback on spectral properties of external cavity semiconductor lasers", Electron. Lett., vol. 20, no. 14, pp. 588-589, 1984.

[20] D. Syvridis, G. Guekos, "Line broadening and intensity noise due to polarization switching in external cavity diode lasers", IEEE Photon. Technol. Lett., vol. 5, no. 2, pp. 151-154, 1993.

[21] D. Mehuys, D. F. Welch, D. R. Scifres, "High-power, diffraction limited, external-cavity tunable diode lasers", LEOS, pp. 598-599, 1993.

[22] C. Etrich, A. W. McCord, P. Mendel, "Dynamical properties of a laser diode with optical feedback from an external high-finesse resonator", IEEE J. off Quantum Electron., vol. 227, no. 4, pp. 937-945, 1991.

[23] H. Asakura, K. Hagiwara, M. Iida, K. Eda, "External cavity semiconductor laser with a Fourier grating and an aspheric lens", Appl. Optics, vol. 32, no. 12, pp. 2031-2038, 1993.

[24] C. J. Corcoran, R. H. Rediker, "The dependence of the output of an external-cavity laser on the relative phases off inputs from five gain elements", IEEE Photon. Technol. Lett., vol. 4, no. 11, 1992.

[25] J.-Y. Kim, H. C. Hsieh, "Asymmetry in the optical output power characteristics of a short-external-cavity laser diode", IEEE Photon. Technol. Lett., vol. 4, no. 6, pp. 537-539, 1992.

[26] J.-Y. Kim, R. W. Chung, J. C. Moulder, "Measurement of photothermally induced distortion of thin films using an external cavity laser diode sensor", Electron. Lett., vol. 29, no. 4, 1993.

[27] J.-Y. Kim, H. C. Hsieh, "An open-resonator model for the analysis of a short external-cavity laser diode and its application to the optical disk head", IEEE J. of Lightwave Technol., vol. 10, no. 4, 1992.

[28] J.-D. Park, D.-S. Seo, J. G. McInerney, "Self-pulsations in strongly coupled asymmetric external cavity semiconductor lasers", IEEE J. of Quantum Mechanics, vol. 26, no. 8, pp. 1353-1361, 1990.

[29] Cerac, "Vacuum Deposition Chemicals, Evaporation Materials", Technical Catalog, Cerac, Third edition, 1988.

[30] H. Ukita, K. Mise, Y. Katagiri, "Simple measurement of the reflectivity of antireflection-coated laser diode facets", Jap. J. of Appl. Physics, vol. 27, no. 6, pp. 1128-1130, 1988.

[31] G. Eisenstein, "Theoretical Design of Single-Layer Antireflection Coatings on Laser Facets", AT&T Bell Lab. Technical Journal, vol. 63, no. 2, pp. 357-364, 1984.

[32] P. Bhattacharya, "Semiconductor Optoelectronic Devices", Prentice Hall, pp. 255-258, 1994.

[33] P. K. Cheo, Handbook of solid-state lasers, "Semiconductor diode lasers", Marcel Dekker Inc., p. 27, eq. 1.41, 1989.

[34] P. K. Cheo, Handbook of solid-state lasers, "Semiconductor diode lasers", Marcel Dekker Inc., p. 35, 1989.

[35] P. K. Cheo, Handbook of solid-state lasers, "Semiconductor diode lasers", Marcel Dekker Inc., p. 30, 1989.

[36] G. A. Alphonse, D. B. Gilbert, M. G. Harvey, M. Ettenberg, "High-power superluminescent diodes", IEEE J. of Quantum Electronics, vol. 24, no. 12, pp. 2454-2457, 1988.

[37] H. C. Casey, M. B. Panish, Quantum Electronics/Principles and Applications, "Heterostructure Lasers", part A: "Fundamental Principles", p. 82-83, 1978.

[38] C. M. Wolfe, N. Holonyak, G. E. Stillman, "Physical properties of semiconductors", Prentice Hall, London, p. 219, eq. 7.87, 1989.

APPENDICES

APPENDIX 1: MATLAB SCRIPTS AND PICTURES

The following MATLAB scripts were written for the determination and analytical calculation of parameters for the antireflection coatings deposited throughout this project.

COATING.M

This program returns the change of reflectivity with coating thickness, where the reflectivity is the square of the absolute value of the reflection coefficient ρ, and ρ is:

$$\rho = \frac{n_2 \cos(kl) + i\, n_3 \sin(kl) - n_2 (n_3 \cos(kl) + i\, n_2 \sin(kl))}{n_2 \cos(kl) + i\, n_3 \sin(kl) + n_2 (n_3 \cos(kl) + i\, n_2 \sin(kl))} \quad \text{where } k = \frac{2\pi n_2}{\lambda_o}.$$

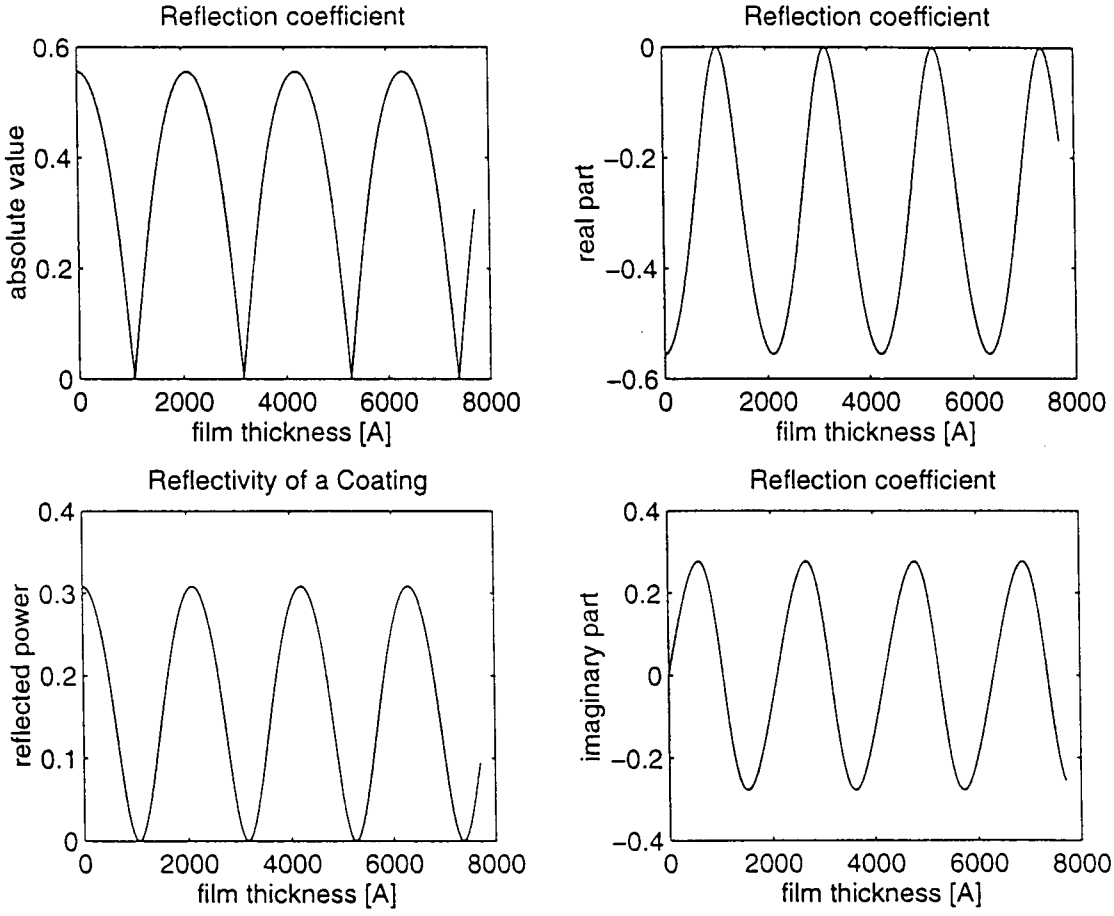

Figure A.1.1.: Output of the MATLAB program "coating.m".

```
%
% coating.m
%
% change of reflectivity with coating thickness
%
% Beate Stephan                          June 14, 1994

clear;
echo off;

n3 = 3.5;

kl = 0:.01:11.5;  % k = 2 pi over lambda, l = thickness %
i  = sqrt(-1);
a  = cos(kl);
b  = sin(kl);
n2 = sqrt(n3);        % n2 of film %
l  = kl*7880/(2*pi*n2);
nx = n2*(n3*a(:)+n2*b(:)*i)./(n2*a(:)+n3*b(:)*i);
     % eta inverse proportional to index %
rhoA = (1-nx);
rhoB = (1+nx);
rho = rhoA./rhoB;
d  = abs(rho);
pow = d.*d;   % fraction of reflected power %
e = real(rho);
f = imag(rho);

clg;
subplot;

subplot(221), plot(l,d);
xlabel(' film thickness [A]');
ylabel('absolute value');
title('Reflection coefficient');

subplot(222), plot(l,e);
xlabel(' film thickness [A]');
ylabel('real part');
title('Reflection coefficient');

subplot(223), plot(l,pow);
xlabel(' film thickness [A]');
ylabel('reflected power');
title('Reflectivity of a Coating');

subplot(224), plot(l,f);
xlabel(' film thickness [A]');
ylabel('imaginary part');
title('Reflection coefficient');
```

THRESHOLD_REFL.M

This program returns the threshold current density of a laser diode with varying reflectivity or varying coating thickness, respectively. The implemented formula is:

$$I_{TH} = A \cdot J_{TH} = A \cdot \frac{8\pi\, q\, d\, \Delta\nu}{\eta_i\, \lambda^2\, \Gamma} \cdot \left(\alpha_i + \frac{1}{2L} \cdot \log(R_1 R_2)^{-1} \right)$$

(see also chapter 4.2). It also calculates the variation of the threshold current with coating thickness and the power output of a laser diode with a threshold current of 40 mA.

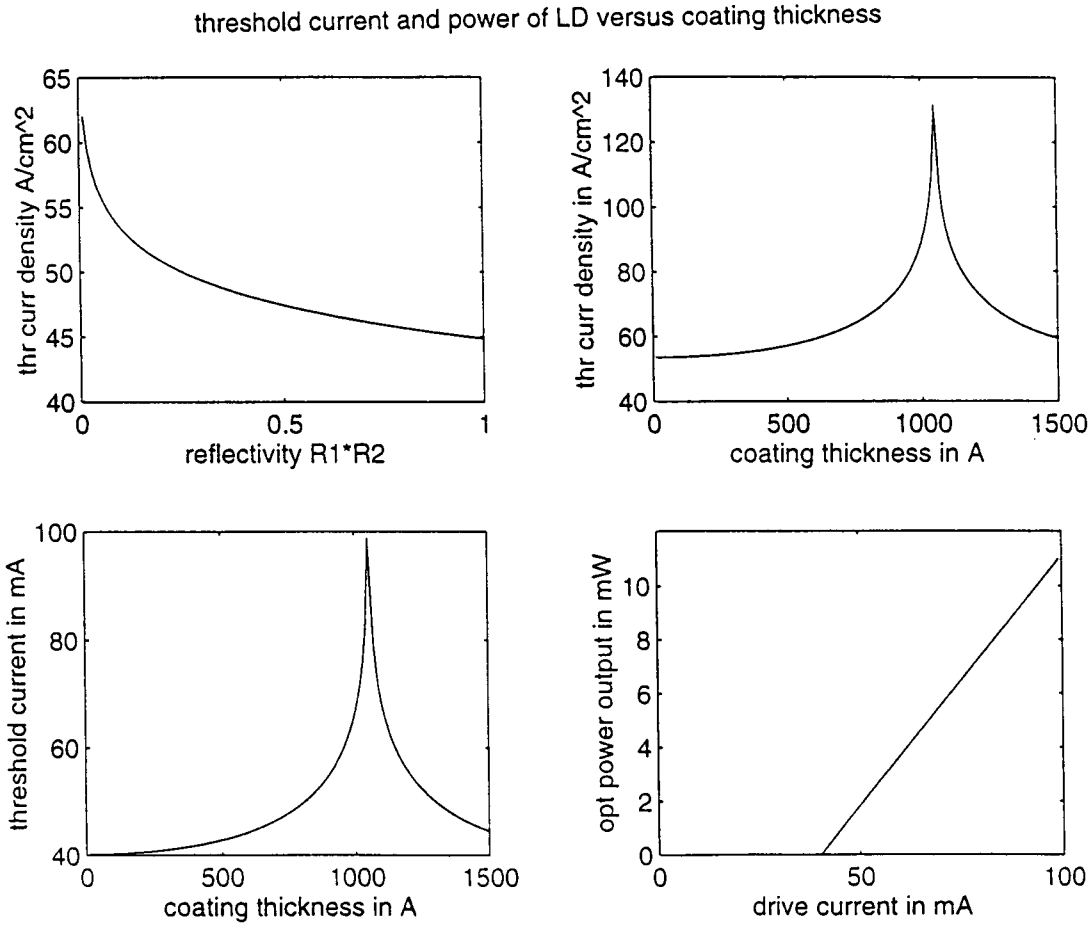

Figure A.1.2.: Output of the MATLAB program "threshold_refl.m".

```
% threshold_refl.m
%
% threshold current density vs. reflectivity and thickness
%
% Beate Stephan                                                    Feb. 26, 94

clear; clg; hold off;

q = 1.6e-19;            % As
d = 100e-9;             % active layer thickness
L = 300e-6;             % cavity length measured
s = 250e-6;             % active layer width
area = L*s;             %
etai = .8;              % approximately
lambda = 788e-9;        %
gamma = .13;            % from Casey and Panish
alphai = 20000;         % m^-1 % 10-15 cm^-1 Cheo or 150-200 cm^-1 from Alphonse
dnu = 3.6e12;           % 3.6e12 measured from LD 7c2 below thr, approx. the same for

c = 8*pi*q*d*dnu/(etai*(lambda^2)*gamma);
r = .01:.01:1;          % r=r1*r2
jth = c * ( alphai + (1/(2*L)) * log(1./r) ); % log = here ln % unit(jth)=A/cm^2
jth = jth/10000;        % unit (jth)=A/cm^2 for the plot

title('threshold current and power of LD versus coating thickness');
subplot(221), plot(r,jth);
title('threshold current and power of LD versus coating thickness');
xlabel('reflectivity R1*R2'); ylabel('thr curr density A/cm^2');

n3 = 3.5;
n2 = sqrt(n3);        % n2 of film %
k = 2*pi*n2/lambda;
l = 10e-10:10e-10:1500e-10;   %k=2pi over lambda, l= coating thickness%
kl = k*l;
j = sqrt(-1);
a = cos(kl); b=sin(kl);
nx = n2*(n3*a+n2*b*j)./(n2*a+n3*b*j); % eta inverse proportional to index %
rhoA = (1-nx); rho8=(1+nx);
rho = rhoA./rho8;
dr = abs(rho);
r1 = dr.*dr;    %fraction of reflected power% r1 or r2
r  = r1.*r1;
jth = c * ( alphai + (1/(2*L)) * log(1./r) ); % (log = ln) in matlab
jth = jth/10000;        % unit(jth)=A/cm^2
l= l*1e10;

subplot(222), plot(l,jth);
xlabel('coating thickness in A'); ylabel('thr curr density in A/cm^2');

jth = jth*10000;        % unit(jth)=A/cm^2*cm^2
ith = jth*area;

ithp = ith * 1000;   % Amps into mA
subplot(223), plot(l,ithp);
xlabel('coating thickness in A'); ylabel('threshold current in mA');
l = l*1e-10;

r = r(1);                              % no coating on either facet
i = ith(1):.001:.1;
c2 = ( (1/(2*L)) * log(1/r) )/( alphai + (1/(2*L)) * log(1/r) );
p = c2*(i(:)-ith(1))*1.42*etai;  % 1.42 = energygap of GaAs at 300K
p = p * 1000;      % Watts into mW
i = i * 1000;      % Amps into mA
subplot(224), plot(i,p); axis([0 100 0 12]); hold on;
xlabel('drive current in mA'); ylabel('opt power output in mW');
```

SINGLE_SIDE_COATING.M

The program "single_side_coating.m" returns the threshold current of a laser diode with coating thickness. It also indicates some of the laser diodes and their coating thickness and threshold after coating.

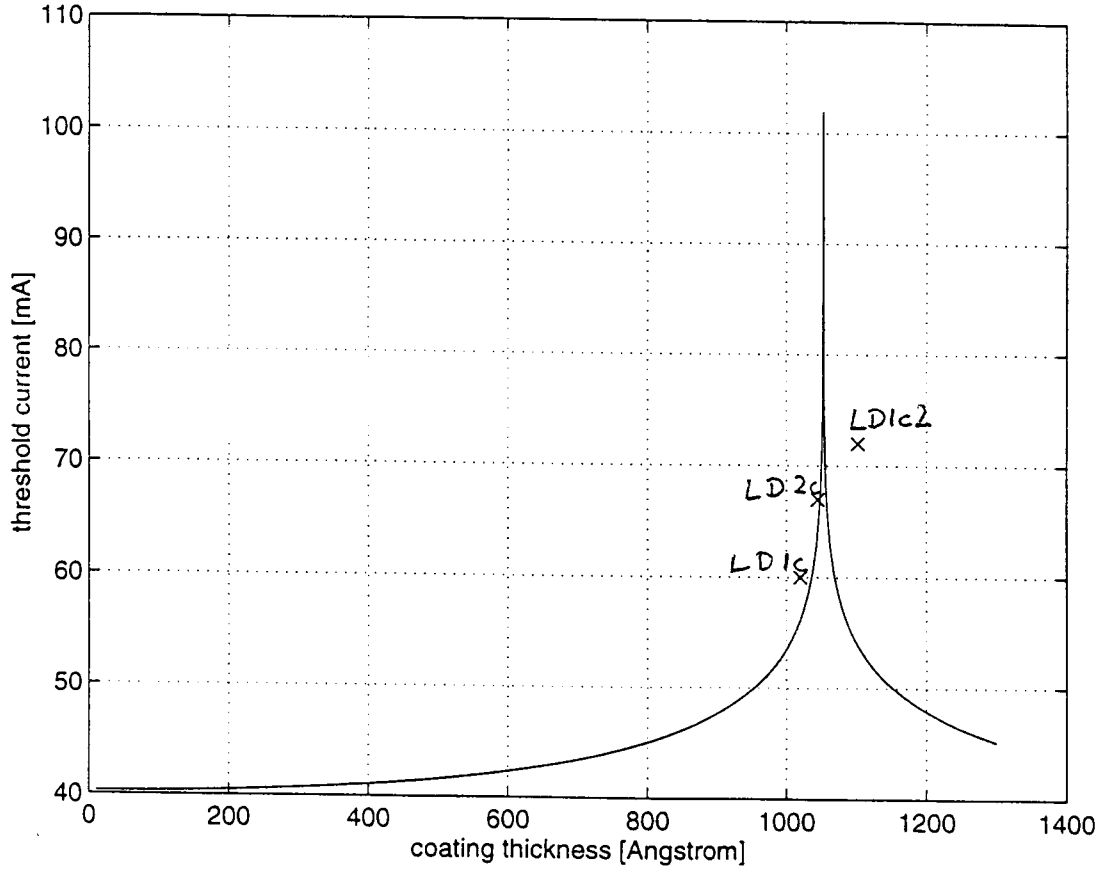

Figure A.1.3.: Output of the MATLAB program "single_side_coating.m".

```
% single_side_coating.m
%
% threshold current vs. thickness and sample coatings
%
% initial threshold = 40 mA single sided coating
%
% Beate Stephan                          Feb 28, 94

clear;
clg;
hold off;

q = 1.6e-19;    % As
d = 100e-7;     % cm = 1000A active layer thickness
L = 300e-4;        % cm  cavity length
s = 250e-4;               % cm  active layer width
etai = .8;              % approx
lambda = 788e-7;        % cm
gamma = .13;       %
alphai = 200;     % 10-15 cm^-1 Cheo or 150-200 from Alphonse
r=.01:.01:1;       % r = r1*r2
dnu = 3.6e12;     %

c = 8*pi*q*d*dnu/(etai*(lambda^2)*gamma);

n3 = 3.5;
n2 = sqrt(n3);        % n2 of film %
k = 2*pi*n2/lambda;
l = 10e-8:1e-8:1300e-8; %cm
% kl = 0:.01:10;  % k = 2 pi over lambda, l = coating thickness %
kl = k*l;
i = sqrt(-1);
a = cos(kl);
b = sin(kl);
nx = n2*(n3*a+n2*b*i)./(n2*a+n3*b*i);
     % eta inverse proportional to index %
rhoA = (1-nx);
rhoB = (1+nx);
rho = rhoA./rhoB;
d = abs(rho);
r1 = d.*d;              % fraction of reflected power % r1 or r2
r2 = .3;
clear r;
r = r1.*r2;

jth = c * ( alphai + (1/(2*L)) * log(1./r) ); % log = here ln % unit(jth)=A/cm^2
ith = jth*(L*s);

l = l * 1e8;                           % cm into Angstroms
ith = ith * 1000;    % Amps into mA
plot(l,ith);
grid;
hold on;
x = [1020,1045,1102];
% x = x*1e-8;                          % cm into A
f = [.060,.067,.072];
f = f * 1000;        % Amps into mA
plot(x,f,'cx');
xlabel('coating thickness [Angstrom]');
ylabel('threshold current [mA]');
```

APPENDIX 2: DIODE FABRICATION

A.2.1. Active material growth with MBE

The first attempt of 788 nm active material was grown at OSU by Molecular Beam Epitaxy (MBE). MBE is a crystal growth technique which is capable of creating very thin layers on planar crystalline substrates. In the case of our AlGaAs laser, gallium and arsenic (and aluminum) are simultaneously deposited onto a heated GaAs substrate. This method enables us to grow quantum well devices. The design for these lasers was a Single Quantum Well (SQW) GRaded INdex (GRIN) structure shown in Figure A.2.1.1. On n+ GaAs a buffer layer of n+ GaAs was grown, followed by the n layer of AlGaAs, the GRIN region of AlGaAs, the quantum well consisting of intrinsic GaAs and of 250 Å thickness, the reciprocal GRIN layer of AlGaAs, the p layer of AlGaAs and a p+ layer of AlGaAs. It is also called a GRINSCH structure, which stands for **GR**aded **IN**dex Separate **C**onfinement **H**eterostructure, since it is a layered structure of two different materials (GaAs and AlGaAs), that is a heterostructure, and since the confinement in the vertical direction is defined by separate means (index guided) from the carrier confinement[37].

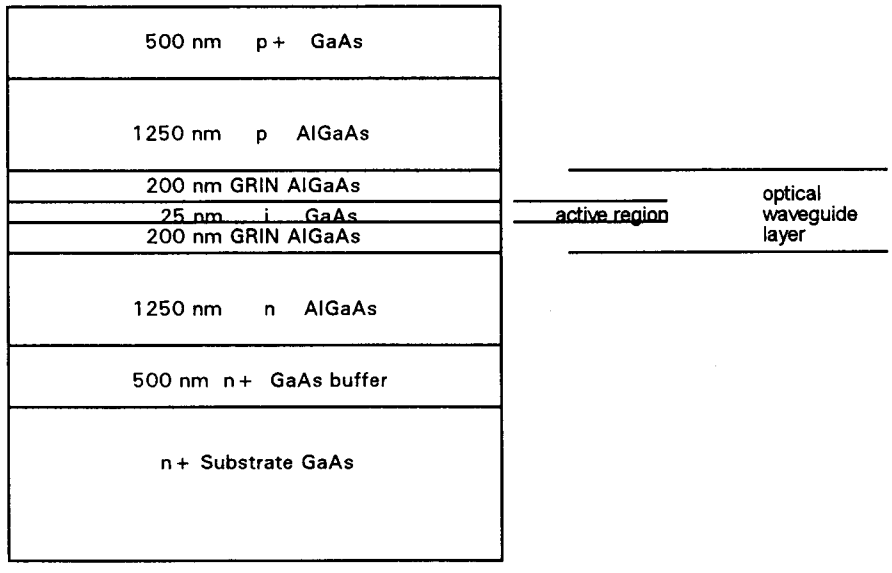

Figure A.2.1.1.: Quantum Well Laser structure grown by MBE at OSU, also showing the separate confining layers for optical and carrier confinement.

The carrier confinement is performed by the active region (here: a quantum well), the optical confinement by the optical waveguide layer. The horizontal confinement is gain guided.

The aluminum mole fraction in the GRIN layer increases from .25 at the quantum well to .5 at the n or p layer, respectively. The purpose of the GRIN regions is to confine the optical output to the active layer. The quantum well is there to analogously provide electrical carrier confinement. The p+ and n+ regions increase the carrier density and decrease the series resistance, thus more current flows at the same drive voltage, which finally means a higher efficiency, since current is directly related to the optical output power.

On the above material the graded index region was manufactured with a ramp function on the temperature control. This induces a roughly linearly varying index profile in the GRIN regions. The energy band diagram will therefore approximately follow the structure in Figure A.2.1.2.

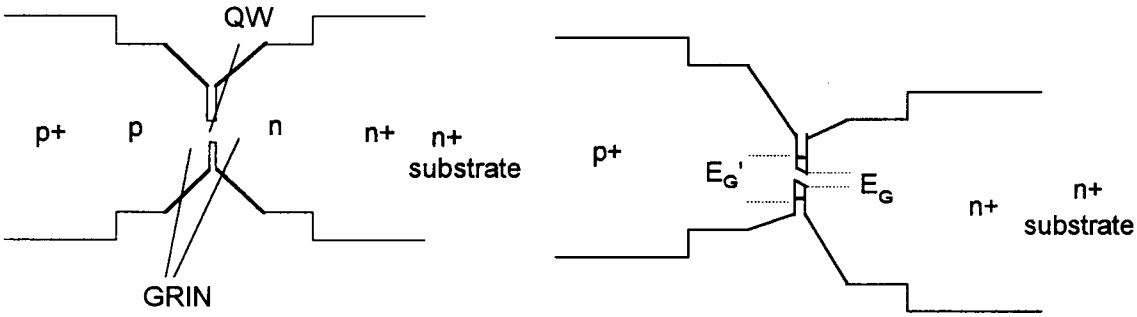

Figure A.2.1.2.: Energy band diagram of the OSU-MBE material under bias (left) and in equilibrium (right).

In this case E_G is the energy gap of GaAs, which is 1.424 eV. The first transition will have the energy of E_G':

$$E_G' = E_G + \frac{h^2 \pi^2}{2m_c L^2} + \frac{h^2 \pi^2}{2m_v L^2}$$

where L is the width of the quantum well, therefore 250 Å in our case. The effective electron mass for GaAs is .067 m_o and the effective light and heavy hole masses are .12 m_o

and .5 m_o, respectively, where m_o is the electron rest mass. The resulting transition energy E_G' is 1.4342 eV from the conduction band to heavy hole (hh) and 1.438 eV from the conduction band to light hole (lh) and the corresponding wavelengths 864.6 nm and 862.3 nm. The second transitions are at $E_G' = 1.48$ eV (lh) and 1.4648 eV (hh) or 846.5 nm (hh) and 837.8 nm (lh). It seems advantageous to design the next MBE material with a narrower quantum well layer for better quantization. Another possibility is to use some 790 nm MOCVD material obtained by UofO with the structure shown in Figure A.2.1.3. The GRIN regions around the quantum well vary the Al concentration from 30 % to 60 % and the 50 nm GRIN buffer region gradually decreases Al to zero at the n+ substrate.

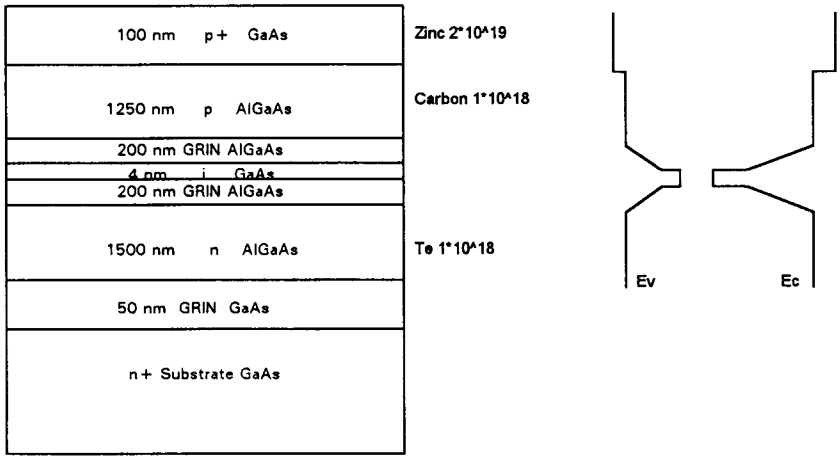

Figure A.2.1.3.: 790 Quantum Well Laser structure grown by UofO and the corresponding energy band structure under bias.

A.2.2. Photoluminescence

To characterize the above MBE GRINSCH material, a photoluminescence spectrum was taken.

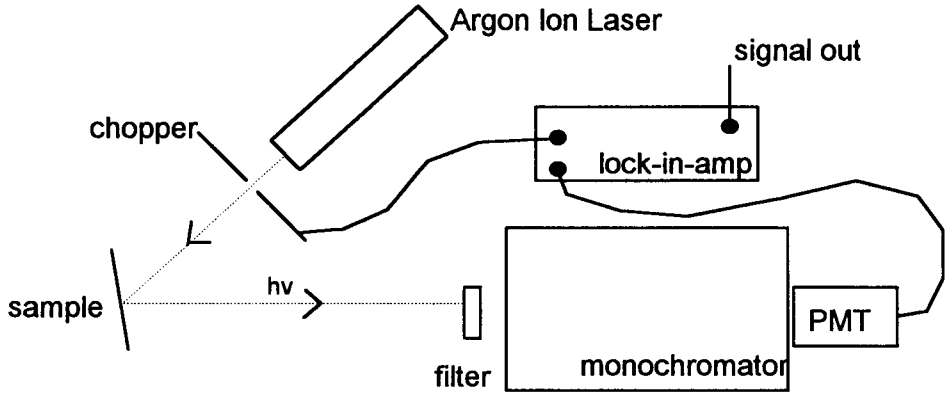

Figure A.2.2.1.: Setup for photoluminescence measurements with 488 nm Argon-ion laser and filter for elimination of the 488 nm signal to the monochromator. The sample is cooled to approx. 20 K while the PMT is cooled to 100 K to reduce the thermal noise.

The photoluminescence measurement of this material grown at OSU was performed using a blue (488 nm) Argon-ion laser by American Laser Corporation and a Jarell-Ash monochromator with a photomultiplier tube (PMT) detector. Figure A.2.2.1 shows the setup for these measurements. The power of the laser can be adjusted from 4 to 30 mW. As can be seen from Figure A.2.2.2, the center frequency is 843 nm and the gain region which is above the noise encompasses some 35 nm. This could provide an excellent external cavity tuning range.

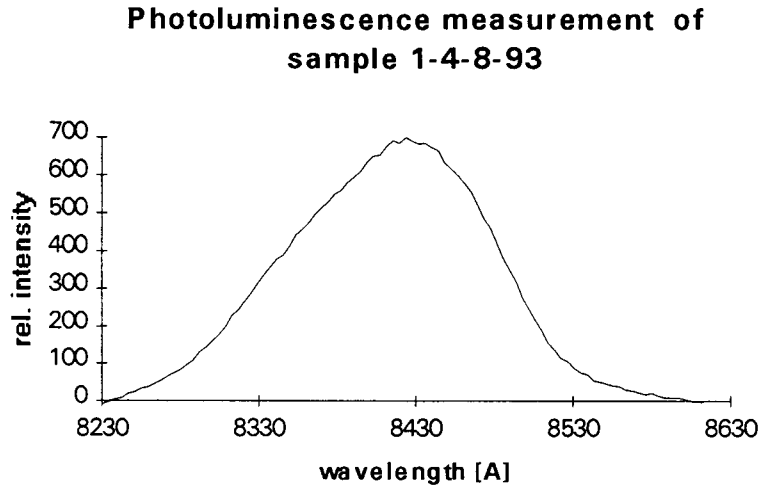

Figure A.2.2.2.: Photoluminescence measurement of GRINSCH laser material 1-4-8-93.

The band structure and thus the band gap of a semiconductor material determines how the material interacts with light and which energy transitions are the most efficient.

The energy gap E_G and therefore the lasing output wavelength λ varies with temperature. As the temperature goes up, the energy gap decreases and the wavelength increases. This measurement was taken at about 20 K, which is an extremely low temperature compared to the operating temperature of laser diodes, which is usually room temperature or just above that. Consequently, the center wavelength will be longer when a processed diode from this material is operated under normal conditions. The band gap energy E_G depends on the temperature T of the material as follows[38]:

$$E_G = 1.522 - \frac{5.8 \cdot 10^{-4}\, T^2}{T + 300} \qquad \text{for GaAs only, T in Kelvin}$$

such that at 0 K, E_G = 1.522 eV or λ=814.7 nm; at 20 K, E_G = 1.52127 eV or λ=815.1 nm and at 300 K (approximately room temperature) E_G = 1.435 eV or λ=864.1 nm. This is a deviation of about 28 nm from the 20 K measured case.

The processed diodes turned out to be of very high series resistance and heated up before they reached the lasing threshold. They could only be used in pulsed operation. A closer look at the p and n buffer layers showed that here might be one of the reasons for the high series resistance, since the doping levels (10^{17}) are lower than usual for similar structures and the layers were fairly thick (1250 nm). A thinner buffer layer might improve the conductivity. Low gold content of the p contact was obviously not the problem as assumed at first, since another processing attempt with thicker gold contacts still rendered a similarly high series resistance. Also, the next MBE material should be fabricated with a narrower quantum well layer for better quantization, because 250 Å is barely enough to impose quantization.

The desired wavelength for the previously mentioned NSF project is the Ti-Sapphire solid state laser wavelength of 810 to 850 nm. The light of the tunable solid state source will be coupled into the TWA to measure quantum noise phenomena. AlGaAs laser structures grown earlier at OSU with an indium concentration in the active region might be used in the continuation of this project, since their wavelength lies in the Ti-Sapphire region.

A.2.3. The processing method

To obtain laser diodes from the active material, the "lift-off process" (see Figure A.2.3.1) was used. It results in a slab of several stripes for active regions that will be cleaved into separate lasers and the desired size of the laser cavity. The lift-off process involves the following steps:

- cleave into 5 mm x 5 mm squares
- deposition of 1000 Å of SiO_2 by means of PECVD
- photolithography for insulating stripes
- photolithography for contact separation
- metal deposition for p contact
- lift-off - Acetone soak (see Figure A.2.3.1, bottom)
- thinning of GaAs to 100 μm (see Figure A.2.3.1, bottom)
- metal deposition for n contact
- cleaving into desired shape

The photolithography involves :

- Clean substrate with Acetone, Methanol, De-ionized water (AMD)
- spin on photoresist (PR) (see Figure A.2.3.1, top)
- soft bake at 85 °C for 25 min.
- expose with mask
- develop 40-60 sec., rinse and blow-dry
- hard bake at 120 °C for 15 min.
- etch in buffered HF to remove SiO_2 in contact stripes (see Figure A.2.3.1, second from top)

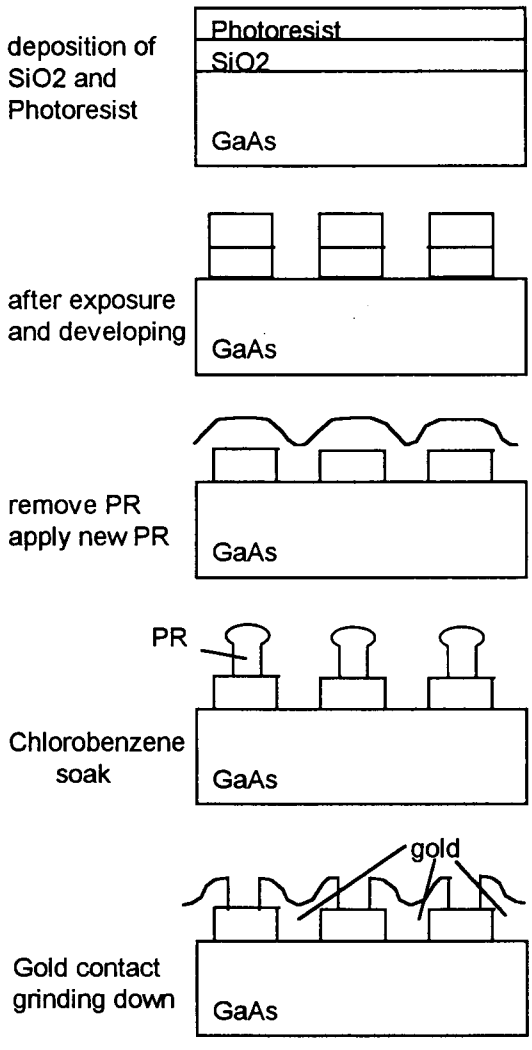

Figure A.2.3.1.: change of the wafer surface during the various steps of photolithography.